

AD-A106 378

DAYTON UNIV OH RESEARCH INST

F/G 11/4

NONLINEAR FINITE ELEMENT ANALYSIS OF SANDWICH COMPOSITES.(U)

MAR 81 R A BROCKMAN

F33615-77-C-3075

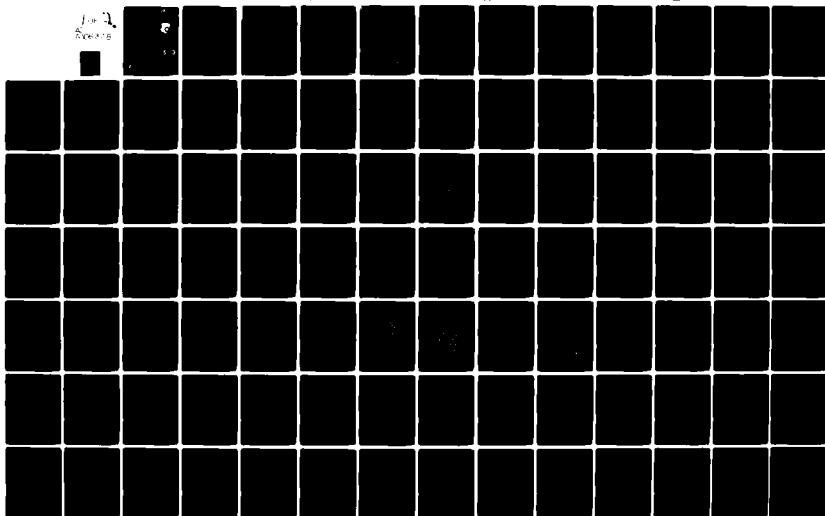
UNCLASSIFIED

UDR-TR-80-113

AFWAL-TR-81-3008

NL

100-1  
100-1



AFWAL-TR-81-3008

② LEVEL II

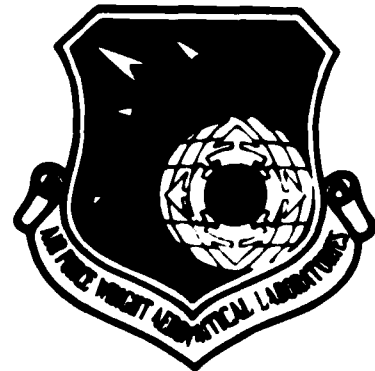
AD A106378

NONLINEAR FINITE ELEMENT ANALYSIS OF SANDWICH COMPOSITES

R. A. Brockman

University of Dayton  
Research Institute  
Dayton, Ohio 45469

March 1981



Final Report for Period September 1977 - November 1980

Approved for public release; distribution unlimited.

DTIC  
ELECTE  
OCT 29 1981  
S B D

DTIC FILE COPY

FLIGHT DYNAMICS LABORATORY  
AIR FORCE WRIGHT AERONAUTICAL LABORATORIES  
AIR FORCE SYSTEMS COMMAND  
WRIGHT-PATTERSON AIR FORCE BASE, OHIO 45433

81 10 28 076

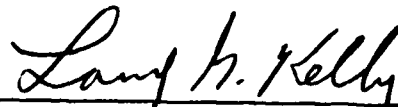
NOTICE

When Government drawings, specifications, or other data are used for any purpose other than in connection with a definitely related Government procurement operation, the United States Government thereby incurs no responsibility nor any obligation whatsoever; and the fact that the government may have formulated, furnished, or in any way supplied the said drawings, specifications, or other data, is not to be regarded by implication or otherwise as in any manner licensing the holder or any other person or corporation, or conveying any rights or permission to manufacture use, or sell any patented invention that may in any way be related thereto.


This report has been reviewed by the Office of Public Affairs (ASD/PA) and is releasable to the National Technical Information Service (NTIS). At NTIS, it will be available to the general public, including foreign nations.

This technical report has been reviewed and is approved for publication.

  
HAROLD C. CROOP, AFWAL/FIBC  
Project Engineer

  
LARRY G. KELLY, Chief,  
Structural Concepts Branch

FOR THE COMMANDER

  
JAMES J. OLSEN, Assistant for  
Research & Technology  
Structures and Dynamics Division

"If your address has changed, if you wish to be removed from our mailing list, or if the addressee is no longer employed by your organization please notify AFWAL/FIBC, WPAFB, Ohio, 45433, to help us maintain a current mailing list".

Copies of this report should not be returned unless return is required by security considerations, contractual obligations, or notice on a specific document.

Unclassified

SECURITY CLASSIFICATION OF THIS PAGE (When Data Entered)

REPORT DOCUMENTATION PAGE		READ INSTRUCTIONS BEFORE COMPLETING FORM
1. REPORT NUMBER AFWAL-TR-81-3008	2. GOVT ACCESSION NO. AD-A106 378	3. RECIPIENT'S CATALOG NUMBER
4. TITLE (and Subtitle) NONLINEAR FINITE ELEMENT ANALYSIS OF SANDWICH COMPOSITES.		5. TYPE OF REPORT & PERIOD COVERED Final Report, September 1977-November 1980
6. PERFORMING ORG REPORT NUMBER UDR-TR-80-133		7. CONTRACT OR GRANT NUMBER(s) F33615-77-C-3075
8. AUTHOR(s) Robert A. Brockman		9. PROGRAM ELEMENT, PROJECT, TASK AREA & WORK UNIT NUMBERS 62201F 2401/83/11
10. CONTROLLING OFFICE NAME AND ADDRESS University of Dayton Research Institute 300 College Park Avenue Dayton, Ohio 45469		11. REPORT DATE March 1981
12. CONTROLLING OFFICE NAME AND ADDRESS Air Force Wright Aeronautical Laboratories AFWAL/FIBCB Wright-Patterson Air Force Base, OH 45433		13. NUMBER OF PAGES 110
14. MONITORING AGENCY NAME & ADDRESS (if different from Controlling Office)		15. SECURITY CLASS. (of this report) Unclassified
16. DISTRIBUTION STATEMENT (of this Report)  Approved for public release; distribution unlimited.		17. SECURITY CLASS. (of the abstract entered in Block 20, if different from Report)
18. SUPPLEMENTARY NOTES		
19. KEY WORDS (Continue on reverse side if necessary and identify by block number)  Sandwich Composite                      Stiffened Panels Finite Elements                              Thin Shells Nonlinear Analysis Buckling		
20. ABSTRACT (Continue on reverse side if necessary and identify by block number)  Finite element analysis techniques are developed for the solution of nonlinear problems involving sandwich composite materials. Each layer of a sandwich panel is represented explicitly so that multicore panels and other configurations are easily considered. The finite element discretization is performed using arbitrary-shaped, fully compatible shell and continuum elements, as well as special elements representing full-depth		

DD FORM 1473 1 JAN 73

EDITION OF 1 NOV 65 IS OBSOLETE

Unclassified

SECURITY CLASSIFICATION OF THIS PAGE (When Data Entered)

Unclassified

SECURITY CLASSIFICATION OF THIS PAGE(When Data Entered)

20. (concluded).

and/or face sheet stiffeners. Each of these elements is capable of representing arbitrarily large displacements and rotations, since no simplifying assumptions are made in the theoretical formulation. Elastic-plastic effects may also be considered. An associated computer program is described which may be used to perform linear or nonlinear solutions for mechanical and thermal loading, linear natural frequency calculations. Several example problems are solved to demonstrate the capabilities of the program.

11

Unclassified

SECURITY CLASSIFICATION OF THIS PAGE(When Data Entered)

## FOREWORD

This report describes work performed by the University of Dayton Research Institute (UDRI) under Air Force Contract F33615-77-C-3075, Structural Sandwich Composites. The effort was conducted for the Flight Dynamics Laboratory, Air Force Wright Aeronautical Laboratories, under the administration and technical direction of the Air Force Project Engineer, Mr. Harold C. Croop (AFWAL/FIBCB).

Administrative project supervision at the UDRI was provided by Mr. Dale H. Whitford (Supervisor, Aerospace Mechanics Division), and technical supervision was provided by Dr. Fred K. Bogner (Group Leader, Analytical Mechanics Group).

Accession For	
NTIS GRA&I	<input checked="checked" type="checkbox"/>
DTIC TAB	<input type="checkbox"/>
Unannounced	<input type="checkbox"/>
Justification	
By	
Distribution/	
Availability Codes	
Avail and/or	
Dist	Special
A	

## TABLE OF CONTENTS

<u>Section</u>		<u>Page</u>
1	INTRODUCTION	1
2	THEORETICAL DEVELOPMENT	3
	2.1 INCREMENTAL EQUATIONS OF MOTION	3
	2.2 CONSTITUTIVE RELATIONS (ELASTIC MATERIALS)	9
	2.3 CONSTITUTIVE RELATIONS (ELASTIC-PLASTIC MATERIALS)	12
3	FINITE ELEMENT APPROXIMATIONS	16
	3.1 THIN SHELL/FACE SHEET ELEMENTS	16
	3.2 SANDWICH CORE ELEMENTS	24
	3.3 STIFFENING MEMBERS	27
	3.4 THREE-DIMENSIONAL SOLID ELEMENTS	30
4	NUMERICAL SOLUTION TECHNIQUES	32
	4.1 STATIC RESPONSE SOLUTION	32
	4.2 NATURAL FREQUENCY SOLUTION	35
5	SAMPLE ANALYSES	38
	5.1 NONLINEAR ANALYSIS OF A SANDWICH PANEL UNDER PRESSURE	38
	5.2 NATURAL FREQUENCIES OF SANDWICH PANELS WITH VARIOUS BOUNDARY CONDITIONS	41
	5.3 STABILITY OF SIMPLY-SUPPORTED SANDWICH PLATE	43
	5.4 PLASTIC ANALYSIS OF A TOROIDAL SANDWICH SHELL	46
	5.5 THERMAL STRESS ANALYSIS OF A VARIABLE-THICKNESS SANDWICH STRIP	50
6	SUMMARY AND CONCLUSIONS	60
APPENDIX:	COMPUTER PROGRAM INPUT DATA	61
REFERENCES		101

## LIST OF ILLUSTRATIONS

<u>Figure</u>		<u>Page</u>
1	Successive States of Deformation for a Three-Dimensional Continuum.	5
2	Shell Element Geometry and Local Coordinates.	18
3	Thin Shell and Sandwich Face Sheet Element.	25
4	Sandwich Core Finite Element.	26
5	Face Sheet Stiffener and Full-Depth Stiffener Element Configurations.	28
6	Stiffener Element Geometry.	29
7	Three-Dimensional Solid Element.	31
8	Newton-Raphson Method for the Solution of Nonlinear Equations.	34
9	Sandwich Panel Under Uniform Lateral Pressure.	39
10	Load-versus-Deflection Curve for Uniformly Loaded Panel.	40
11	Three-Layer Sandwich Panel used in Natural Frequency Calculations.	42
12	Simply Supported Sandwich Panel Under Edge Compression.	45
13	Toroidal Sandwich Shell.	48
14	Upper Face Sheet of Toroidal Shell Panel with Node Numbers.	49
15	Deformed Shape of Inner Face Sheet at Maximum Loading.	52
16	Deformed Shape of Outer Face Sheet at Maximum Loading.	53
17	Plastic Boundary in Outer Face Sheet of Toroidal Shell at Maximum Load.	54
18	Asymmetric Sandwich Strip.	55

LIST OF ILLUSTRATIONS (CONTINUED)

<u>Figure</u>		<u>Page</u>
19	Face Sheet and Stiffener Elements in Sandwich Strip Model.	57
20	Core Elements in Sandwich Strip Model.	58
21	Displaced Shape of Heated Sandwich Strip.	59
A.1	Orthotropic Axis Definition.	75
A.2	Connectivity for Sandwich Core Element.	77
A.3	Connectivity for Stiffener Elements.	81
A.4	Connectivity for Thin Shell/Face Sheet Element.	86
A.5	Connectivity for 3-D Solid Element.	93

## LIST OF TABLES

<u>Table</u>		<u>Page</u>
1	NATURAL FREQUENCY RESULTS FOR FLAT SANDWICH PANEL WITH VARIOUS BOUNDARY CONDITIONS	44
2	COMPARISON OF BUCKLING LOADS FOR SIMPLY-SUPPORTED SANDWICH PANEL	47
3	LOAD-DEFLECTION HISTORY AT CENTRAL POINT ON LOADED EDGE OF TOROIDAL SANDWICH PANEL	51

## SECTION 1

### INTRODUCTION

Sandwich composites constitute an important class of materials in the aerospace and building industries due to their potential to provide high resistance to loading at a relatively low weight penalty. Typical uses of sandwich materials presently include wing skins and control surfaces, fairings, shelving, cargo doors, helicopter blades, and prefabricated panels for building construction.

As the application of these advanced materials increases, sophisticated analysis techniques become increasingly important for use in the formulation and qualification of practical designs. The necessary analytical methods must be readily accessible to the designer, while remaining quite general in scope. To achieve the objective of generality, computational methods must be employed, the most flexible of these being techniques based upon finite element<sup>1</sup> discretization.

The development of finite element analysis techniques applicable to sandwich constructions is complicated by the nature of the response of most sandwich layups. The relatively thin, high-modulus face sheet layers resist loading through inplane stresses, and thus are represented most effectively with plate or shell type elements. Sandwich core, which is typically much thicker and more flexible than the face sheets, deforms principally in transverse shear modes, and therefore, is modeled most appropriately by three-dimensional, shear-deformable elements. The incompatibility of these two classes of finite elements (shells and solids) is well-known, and a departure from the traditional elements of these types is clearly necessary. A number of specialized formulations have been proposed to deal with the modeling problems of sandwich materials<sup>2-6</sup>. However, none of these has been developed in sufficient generality to provide truly comprehensive modeling

capabilities for sandwich panels having arbitrary curvature, multicore construction, transitions to other types of structure, edge closeouts, and other troublesome geometrical features. Applications to nonlinear sandwich analysis, including finite displacements, large rotations, and material nonlinearities are typically further restricted (flat panels, single-core sandwich, or rectangular shapes) due to the complexity of the formulation and long solution times.

The present report documents a finite element approach for the analysis of sandwich structures of arbitrary geometry, which may include stiffening members, closeouts, and connections to other three-dimensional structural components. Static response to mechanical and thermal loading may be computed for either linear or nonlinear deformations. In the case of nonlinear analysis, arbitrarily large displacements and rotations are permitted, in addition to material nonlinearities (plasticity). Linear natural frequency and normal mode calculations can also be performed.

## SECTION 2

### THEORETICAL DEVELOPMENT

The basis of the present analysis of sandwich materials is the incremental equilibrium relation for a general, three-dimensional continuum experiencing large displacements and materially nonlinear response. Each of the finite elements (face sheet, core, stiffener, solid) described in Section 3 is derived from this general set of governing equations by first making appropriate specializations and then applying the procedure of finite element discretizations.

For finite element application, the appropriate form of the equilibrium equations is expressed in terms of the principle of virtual work. In this Section, the incremental form of the principle of virtual work is obtained for a general, three-dimensional continuum. The Lagrangian description of motion is used throughout: that is, all displacements, strains and stresses are expressed in terms of the original (undeformed) configuration of the body. The appropriate constitutive relations for elastic and elastic-plastic material behavior are also developed.

#### 2.1 INCREMENTAL EQUATIONS OF MOTION

For the purpose of obtaining an incremental description of motion, three configurations of a general structure are considered:

- Configuration  $C^0$  : the initial state of the body, used as a reference state
- Configuration  $C^1$  : an intermediate state, at which a solution for the structural response is assumed to be known
- Configuration  $C^2$  : a subsequent configuration, removed from state  $C^1$  by a single increment of loading.

These three states of deformation are shown in Figure 1. In an incremental nonlinear analysis, the objective at each step of the solution is to compute a configuration such as  $C^2$ , given the previous solution (state  $C^1$ ) and the incremental values of mechanical and thermal loading.

In the initial state  $C^0$ , the position of an arbitrary point P (Figure 1) is denoted by  $X_i$ ;  $i=1,2,3$ . In reaching configuration  $C^1$ , the point P moves to a new position whose coordinates are  $x_i$ , where

$$x_i = X_i + {}_1u_i \quad (1)$$

and  ${}_1u_i$  represent the displacements in state  $C^1$ . The state of strain at state  $C^1$  is measured by the Green-St. Venant strain tensor<sup>7</sup>

$${}_1e_{ij} = \frac{1}{2}({}_1u_{i,j} + {}_1u_{j,i} + {}_1u_{k,i} {}_1u_{k,j}). \quad (2)$$

Observe that, in Equation 2, differentiation is performed with respect to the initial coordinates  $X_i$ ; that is,

$${}_1u_{i,j} \equiv \frac{\partial}{{}_1u_i / \partial X_j}. \quad (3)$$

The appropriate measure of the stress corresponding to Equation 2 are

$${}_1s_{ij} = \sqrt{G} {}_1\Pi_{ij} \quad (4)$$

where  ${}_1\Pi_{ij}$  are the symmetric Piola-Kirchoff stresses<sup>7</sup> in configuration  $C^1$ , and  $\sqrt{G}$  is the determinant of the Green's deformation tensor

$$G = \left| \frac{\partial x_i}{\partial X_j} \right|^2. \quad (5)$$

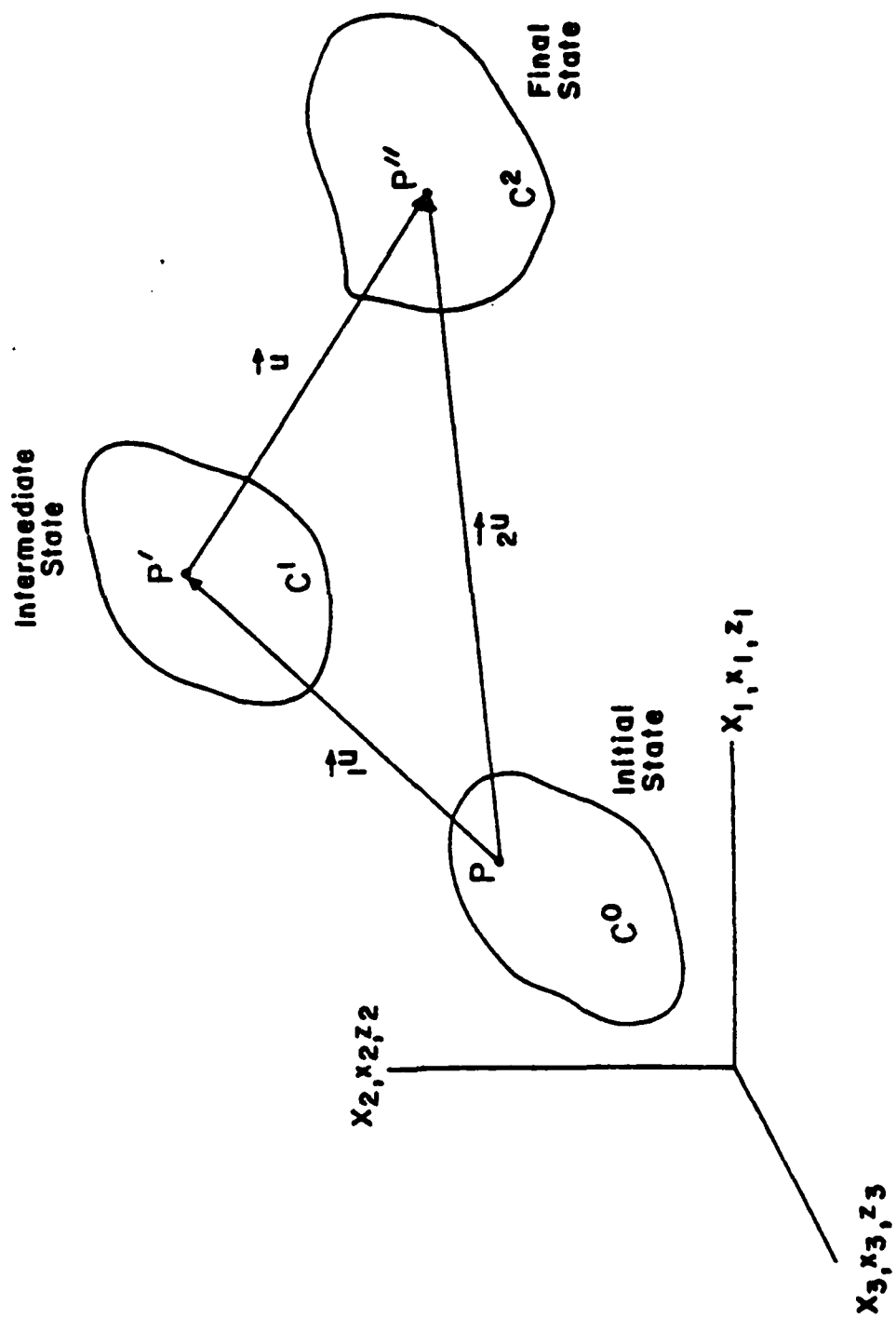


Figure 1. Successive States of Deformation for a Three-Dimensional Continuum.

Similarly in configuration  $C^2$ , denote the position of the point P by coordinates  $z_i$ ;  $i=1,2,3$ . Then

$$z_i = x_i + {}_2u_i = x_i + \Delta u_i \quad (6)$$

in which  $\Delta u_i$  are incremental displacements separating the states  $C^1$  and  $C^2$ . The strain and stress are

$${}_2e_{ij} = {}_1e_{ij} + \Delta e_{ij} \quad (7)$$

and

$${}_2s_{ij} = {}_1s_{ij} + \Delta s_{ij} \quad (8)$$

respectively.

Next consider the principle of virtual work<sup>7</sup> in configurations  $C^1$  and  $C^2$ , which are written

$$\int_{{}_0V} {}_1s_{ij} x_{k,i} \delta u_{k,j} dV = \int_{{}_0\partial V} {}_1\bar{t}_i \delta u_i dA \quad (9)$$

and

$$\int_{{}_0V} {}_2s_{ij} z_{k,i} \delta u_{k,j} dV = \int_{{}_0\partial V} {}_2\bar{t}_i \delta u_i dA \quad (10)$$

Here  ${}_0V$  represents the original volume of the body (in state  $C^0$ ),  ${}_0\partial V$  denotes the corresponding boundary surface, and  ${}_1\bar{t}_i$ ,  ${}_2\bar{t}_i$  are the prescribed surface forces in states  $C^1$  and  $C^2$  respectively. It is important to notice that the virtual displacements  $\delta u_i$  may be any kinematically admissible displacements, and that they are measured in each case with respect to the initial configuration. Thus by subtracting Equations 9 and 10 it is possible to write

$$\int_V (2s_{ij}z_{k,i} - 1s_{ij}x_{k,i}) \delta u_{k,j} dV = \int_{\partial V} \bar{\Delta t}_i \delta u_i dA \quad (11)$$

where  $\bar{\Delta t}_i$  are the increments in prescribed surface traction,

$$\bar{\Delta t}_i = 2\bar{t}_i - 1\bar{t}_i. \quad (12)$$

Using the incremental stresses defined in Equation 8, Equation 11 can be arranged in the form

$$\int_V (1s_{ij}\Delta u_{k,i} + \Delta s_{ij}z_{k,i}) \delta \Delta u_{k,j} dV = \int_{\partial V} \bar{\Delta t}_i \delta \Delta u_i dA \quad (13)$$

Note that the arbitrary virtual displacements  $\delta u_i$  have been replaced by incremental virtual displacements  $\delta \Delta u_i$ , which is clearly admissible provided both sets of virtual displacements satisfy the imposed kinematic boundary conditions of the problem.

Equation 13 expresses the equality of internal and external virtual work performed during the increment of deformation between configurations  $C^1$  and  $C^2$ . Using Equation 6, the equation obtained above can be expressed more conveniently in terms of the incremental strains  $\Delta e_{ij}$  (Equation 7). Since the incremental stress tensor  $\Delta s_{ij}$  is symmetric,

$$\Delta s_{ij}z_{k,i}\delta \Delta u_{k,j} = \frac{1}{2} \Delta s_{ij} (z_{k,i}\delta \Delta u_{k,j} + z_{k,j}\delta \Delta u_{k,i}) \quad (14)$$

and thus

$$\Delta s_{ij}z_{k,i}\delta \Delta u_{k,j} = \Delta s_{ij}\delta \Delta e_{ij}. \quad (15)$$

The incremental principle of virtual work, Equation 13, then becomes

$$\int_0^V (\Delta s_{ij} \delta \Delta e_{ij} + l s_{ij} \Delta u_{k,i} \delta \Delta u_{k,j}) dv = \int_0^{\partial V} \overline{\Delta \epsilon}_i \delta \Delta u_i dA. \quad (16)$$

For later use, it is useful to separate those terms of the incremental strain  $\Delta e_{ij}$  which are linear and nonlinear in the incremental displacements  $\Delta u_i$ .

Define

$$\Delta e_{ij} = \Delta \epsilon_{ij} + \Delta \eta_{ij} \quad (17)$$

in which

$$\Delta \epsilon_{ij} = \frac{1}{2} (\Delta u_{i,j} + \Delta u_{j,i} + l u_{k,i} \Delta u_{k,j} + l u_{k,j} \Delta u_{k,i}) \quad (18)$$

$$\Delta \eta_{ij} = \frac{1}{2} \Delta u_{k,i} \Delta u_{k,j}. \quad (19)$$

Equation (17) becomes

$$\int_0^V (\Delta s_{ij} \delta \Delta e_{ij} + l s_{ij} \delta \Delta \eta_{ij}) dv = \int_0^{\partial V} \overline{\Delta \epsilon}_i \delta \Delta u_i dA \quad (20)$$

The material stress-strain relation used here assumes that the incremental stresses and strains can be related in a linear fashion,

$$\Delta s_{ij} = D_{ijkl} (\Delta e_{ij} - \alpha_{kl} \Delta T). \quad (21)$$

Here  $\alpha_{kl}$  are the thermal expansion coefficients and  $\Delta T$  is an incremental change in temperature at a point. Combining Equations 20 and 21 yields the final form of the incremental principle of virtual work,

$$\int_0^V [D_{ijkl} (\Delta e_{kl} - \alpha_{kl} \Delta T) \delta \Delta e_{ij} + s_{ij} \delta \Delta \eta_{ij}] dv = \int_0^{\partial V} \Delta t_i \delta \Delta u_i dA. \quad (22)$$

Equation 22 is fully three-dimensional, and specific forms which are used to derive the individual finite element types are discussed in Section 3. The iterative solution of Equation 22, which is nonlinear, is outlined in Section 4.

## 2.2 CONSTITUTIVE RELATIONS (ELASTIC MATERIALS)

For elastic materials, the incremental stress-strain law of Equation 21 is precisely the same as the relation between total stresses and strains,

$$s_{ij} = D_{ijkl} (e_{kl} - \alpha_{kl} T), \quad (23)$$

where  $T$  is interpreted as the temperature change from a fixed reference temperature. In matrix form, Equation 23 can be written as

$$\underline{s} = \underline{D} (\underline{e} - \underline{\alpha} T) \quad (24)$$

in which

$$\underline{s}^T = [s_{11} \ s_{22} \ s_{33} \ s_{23} \ s_{13} \ s_{12}] \quad (25)$$

$$\underline{e}^T = [e_{11} \ e_{22} \ e_{33} \ e_{23} \ e_{13} \ e_{12}] \quad (26)$$

$$\underline{\alpha}^T = [\alpha_{11} \alpha_{22} \alpha_{33} \alpha_{23} \alpha_{13} \alpha_{12}] \quad (27)$$

and  $\underline{D}$  is a coefficient matrix of order six.

In the case of an isotropic material,  $\underline{D}$  is completely determined by the values of Young's modulus  $E$  and the Poisson's ratio  $\nu$ ,

$$\underline{D} = \frac{E}{(1+\nu)(1-2\nu)} \begin{bmatrix} (1-\nu) & \nu & \nu & 0 & 0 & 0 \\ \nu & (1-\nu) & \nu & 0 & 0 & 0 \\ \nu & \nu & (1-\nu) & 0 & 0 & 0 \\ 0 & 0 & 0 & (\frac{1-2\nu}{2}) & 0 & 0 \\ 0 & 0 & 0 & 0 & (\frac{1-2\nu}{2}) & 0 \\ 0 & 0 & 0 & 0 & 0 & (\frac{1-2\nu}{2}) \end{bmatrix} \quad (28)$$

and  $\alpha$  depends only upon the scalar coefficient of thermal expansion,  $\alpha$ :

$$\underline{\alpha}^T = [\alpha \quad \alpha \quad \alpha \quad 0 \quad 0 \quad 0] . \quad (29)$$

For orthotropic materials, the elastic properties are direction-dependent, and a stress-strain law must first be formulated with respect to the preferential axes of the material, and then transformed to global coordinates. In the material coordinate system (denoted by a subscript  $m$ ), Equation 25 becomes

$$\underline{s}_m = \underline{D}_m (\underline{e}_m - \underline{\alpha}_m T) . \quad (30)$$

The matrix  $\underline{D}_m$  is a function of nine independent material constants: the extensional moduli  $E_1, E_2, E_3$ ; the Poisson's Ratios  $\nu_{23}, \nu_{13}, \nu_{12}$ ; and the shear moduli  $G_{23}, G_{13}, G_{12}$ . The

nonzero upper triangular elements of  $D_m$ , which is symmetric, are given by<sup>8</sup>

$$\begin{aligned}
 d_{11} &= (1 - \nu_{23}\nu_{32})E_1/N \\
 d_{12} &= (\nu_{12} + \nu_{32}\nu_{13})E_2/N \\
 d_{13} &= (\nu_{13} + \nu_{12}\nu_{23})E_3/N \\
 d_{22} &= (1 - \nu_{13}\nu_{32})E_2/N \\
 d_{23} &= (\nu_{23} + \nu_{21}\nu_{13})E_3/N \\
 d_{33} &= (1 - \nu_{12}\nu_{21})E_3/N \\
 d_{44} &= G_{23} \\
 d_{55} &= G_{13} \\
 d_{66} &= G_{12}
 \end{aligned} \tag{31}$$

in which

$$N = 1 - \nu_{12}\nu_{21} - \nu_{23}\nu_{32} - \nu_{31}\nu_{13} - 2\nu_{21}\nu_{32}\nu_{13}. \tag{32}$$

It should be noted that the material properties in Equations 31 must satisfy certain constraints in order to be valid from symmetry and energy considerations. These constraints can be summarized as follows<sup>8</sup>:

$$E_i > 0 \tag{33}$$

$$G_{ij} > 0 \tag{34}$$

$$(1 - v_{ij} v_{ji}) > 0 \quad (\text{no sum}) \quad (35)$$

$$\frac{v_{ij}}{E_i} = \frac{v_{ji}}{E_j} \quad (36)$$

$$N > 0. \quad (37)$$

With respect to the global coordinates of a body, the stress-strain relation in Equation 30 becomes

$$\underline{\underline{S}} = \underline{\underline{T}}_s \underline{\underline{D}}_m \underline{\underline{T}}_e^t (\underline{\underline{e}} - \underline{\underline{T}}_e^{-t} \underline{\underline{\alpha}}_m \underline{\underline{T}}). \quad (38)$$

Here  $\underline{\underline{T}}_s$ ,  $\underline{\underline{T}}_e$  define the transformations for stress and strain between the material and global axes:

$$\underline{\underline{S}} = \underline{\underline{T}}_s \underline{\underline{s}}_m \quad (39)$$

$$\underline{\underline{e}} = \underline{\underline{T}}_e \underline{\underline{e}}_m. \quad (40)$$

A comparison of Equations 23 and 38 yields the correct transformations needed for  $\underline{\underline{D}}_m$  and  $\underline{\underline{\alpha}}_m$ , namely

$$\underline{\underline{D}} = \underline{\underline{T}}_s \underline{\underline{D}}_m \underline{\underline{T}}_e^t \quad (41)$$

$$\underline{\underline{\alpha}} = \underline{\underline{T}}_e^{-t} \underline{\underline{\alpha}}_m. \quad (42)$$

### 2.3 CONSTITUTIVE RELATIONS (ELASTIC-PLASTIC MATERIALS)

The elastic-plastic material law considered in the present development, which is applicable to initially isotropic materials, is based upon the von Mises yield criterion<sup>9</sup>,

$$F(s_{ij}) = \frac{3}{2} s'_{ij} s'_{ij} = k^2 \quad (43)$$

in which  $s'_{ij}$  represent the deviatoric stresses

$$s'_{ij} = s_{ij} - \frac{1}{3}s_{kk}\delta_{ij}$$

and  $k^2$  represents the diameter of the yield surface. For this yield function, the associated plastic flow rule is

$$\dot{e}_{ij}^p = \lambda \frac{\partial F}{\partial s_{ij}} \quad (44)$$

or, from Equation 43,

$$\dot{e}_{ij}^p = 3\lambda s'_{ij} \quad (45)$$

That is, the individual components of the plastic strain rate are proportional to the corresponding deviatoric stresses.

The consistency condition is used in the form noted by Hunsaker<sup>10</sup> to obtain a computationally effective procedure. Thus

$$\frac{\partial F}{\partial s_{ij}} \dot{s}_{ij} = H \frac{\partial F}{\partial s_{ij}} \dot{e}_{ij}^p \quad (46)$$

The parameter  $H$  characterizes the strain-hardening slope of the stress-strain curve, and in the one dimensional case reduces to

$$H = \frac{E E_T}{E - E_T} \quad (47)$$

in which  $E_T$  is the tangent to the uniaxial stress-strain curve.

Finally, assuming an additive decomposition of the strain rates into elastic and plastic components gives

$$\dot{s}_{ij} = E_{ijkl} (\dot{e}_{kl} - \dot{e}_{kl}^p). \quad (48)$$

Here  $E_{ijkl}$  is the modulus tensor of the material in its elastic state. Combining Equations 44, 46 and 48 permits a solution for  $\lambda$  in terms of the total strain rate,

$$\lambda = \frac{E_{ijkl} \frac{\partial F}{\partial S_{ij}} \dot{e}_{kl}}{(E_{ijkl} \frac{\partial F}{\partial S_{kl}} + H \frac{\partial F}{\partial S_{ij}}) \frac{\partial F}{\partial S_{ij}}} \quad (49)$$

Eliminating  $\lambda$  in the expression for  $\dot{e}_{kl}^P$  in Equation 48 then leads to the rate relation

$$\dot{s}_{ij} = D_{ijkl} \dot{e}_{kl} \quad (50)$$

where the tensor  $D_{ijkl}$  is given by

$$D_{ijkl} = E_{ijkl} - \beta S_{ij} S_{kl} \quad (51)$$

and

$$\beta = \left\{ \begin{array}{ll} 0, & \text{(elastic)} \\ 3G/(1+H/2G)k^2 & \text{(plastic)} \end{array} \right\}. \quad (52)$$

It remains to determine the expansion of the yield surface as plastic flow progresses in a strain-hardening material. This information is obtained by requiring that any point in stress space remain on the yield surface during inelastic deformation (that is, that Equation 44 always be satisfied). If the stress rate  $\dot{s}_{ij}$  are known, then

$$\dot{k} = \frac{1}{2k} \frac{\partial F}{\partial S_{ij}} \dot{s}_{ij}. \quad (53)$$

In practice, the elastic-plastic constitutive equation must be integrated to give the desired relationship between

stress and strain increments (see Equation 22). In the present formulation this integration is performed using a trapezoidal rule over a number of strain subincrements whose size is controlled to preserve accuracy. During any subincrement, then Equations 50 and 53 become

$$\Delta s_{ij} = (E_{ijkl} - \beta s'_{ij} s'_{kl}) \Delta e_{kl} \quad (54)$$

and

$$\Delta k = \frac{3}{2k} s'_{ij} \Delta s_{ij}. \quad (55)$$

Depending upon the size of the computed strain increment, Equations 54 and 55 may be applied tens or even hundreds of times in succession to update the element stress state with an acceptable degree of accuracy.

### SECTION 3

#### FINITE ELEMENT APPROXIMATIONS

The present development includes four classes of finite element approximations: thin shell or sandwich face sheet, sandwich core; stiffening members; and general, three-dimensional solids. The first three of these finite element types are most often used specifically for modeling the individual components of stiffened sandwich panels, while the solid element is used for other structure, for connections between sandwich and other components, and for more detailed analysis of sandwich constructions themselves.

Each of the finite element approximations described in this Section is obtained from the nonlinear equilibrium of Section 2 by appropriate specialization. Linear forms of the governing equations are also obtained from the general formulation through the assumptions of infinitesimal displacements and elastic material response.

#### 3.1 THIN SHELL/FACE SHEET ELEMENTS

The formulation of Reference 11 is used herein to obtain a thin plate and shell finite element suitable for representing sandwich face sheet materials. This element is based upon a penalty function formulation, which leads to an effective thin shell approximation derived directly from the field equations of a three-dimensional continuum. The shell element so derived possesses several distinct advantages over similar elements based upon a specific theory of thin shells. In particular,

- geometric parameters of an element are completely defined by the nodal coordinate information,
- complete compatibility of displacements with standard isoparametric solid elements is possible,
- no restrictions need be placed upon the extent of displacements or rotations of the shell, and

- effects such as variable thickness, complex shell intersections, skewed lateral boundaries and connections to adjacent structure are accounted for simply and effectively.

The undeformed geometry of a single element of a shell (or face sheet) is shown in Figure 2. Geometric parameters are analyzed with respect to a local coordinate system  $(x,y)$  which is close to the element midsurface  $z = z(x,y)$  at all points. An additional coordinate  $\zeta$  is used to describe the distance away from the midsurface at any point.

It is assumed that on the element level, the shell is shallow, so that

$$\begin{aligned} z_{,x}^2 &\ll 1 \\ z_{,y}^2 &\ll 1 \end{aligned} \quad (56)$$

everywhere. The unit vector normal to the shell midsurface at a point can then be written as

$$\hat{n} = -z_{,x}\hat{i} - z_{,y}\hat{j} + \hat{k} \quad (57)$$

in the local system of coordinates. Due to the assumption of shallowness, the  $(x,y,\zeta)$  coordinates constitute, at least approximately, a local Cartesian system; taking advantage of this fact, the position vectors of an arbitrary point within the shell before and after deformation may be expressed in the form

$$\vec{r} = (x - \zeta z_{,x})\hat{i} + (y - \zeta z_{,y})\hat{j} + (z + \zeta)\hat{k} \quad (58)$$

and

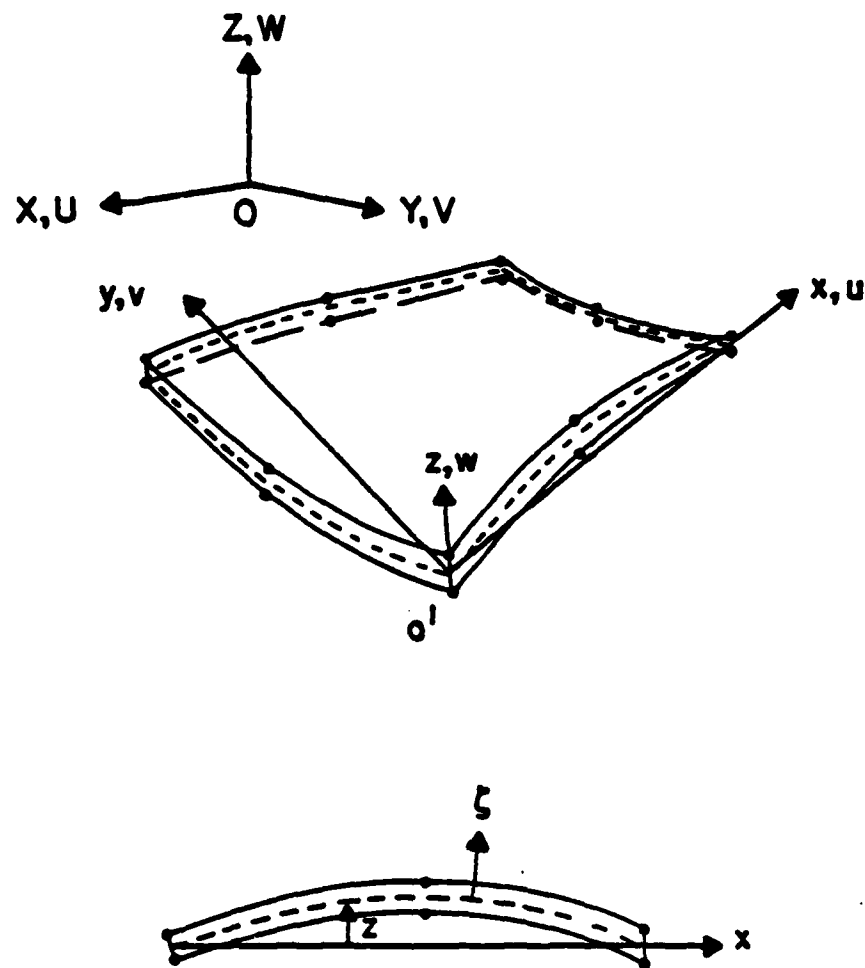


Figure 2. Shell Element Geometry and Local Coordinates.

$$\begin{aligned}\vec{R} = & (x - \zeta z_{,x} + u)\hat{i} + (y - \zeta z_{,y} + v)\hat{j} \\ & + (z + \zeta + w)\hat{k}.\end{aligned}\quad (59)$$

Equations 58 and 59 lead directly to the appropriate definitions of strain for the shell element, since<sup>12</sup>

$$e_{ij}dx_i dx_j = \frac{1}{2}[(\vec{dR} \cdot \vec{dR}) - (\vec{dr} \cdot \vec{dr})]. \quad (60)$$

Thus, the Green's strains referred to the system  $(x, y, \zeta)$  become:

$$\begin{aligned}e_{xx} = & u_{,x}(1 - \zeta z_{,xx}) - \zeta z_{,xy}v_{,x} + z_{,x}w_{,x} \\ & + \frac{1}{2}(u_{,x}^2 + v_{,x}^2 + w_{,x}^2)\end{aligned}$$

$$\begin{aligned}e_{yy} = & v_{,y}(1 - \zeta z_{,yy}) - \zeta z_{,xy}u_{,y} + z_{,y}w_{,y} \\ & + \frac{1}{2}(u_{,y}^2 + v_{,y}^2 + w_{,y}^2)\end{aligned}$$

$$\begin{aligned}e_{\zeta\zeta} = & w_{,\zeta} - z_{,x}u_{,\zeta} - z_{,y}v_{,\zeta} \\ & + \frac{1}{2}(u_{,\zeta}^2 + v_{,\zeta}^2 + w_{,\zeta}^2)\end{aligned}$$

$$\begin{aligned}2e_{y\zeta} = & v_{,\zeta}(1 - \zeta z_{,yy}) + w_{,y} - z_{,x}u_{,y} + z_{,y}(w_{,\zeta} - v_{,y}) \\ & - \zeta z_{,xy}u_{,\zeta} + u_{,y}u_{,\zeta} + v_{,y}v_{,\zeta} + w_{,y}w_{,\zeta}\end{aligned}$$

$$\begin{aligned}
2e_{x\zeta} &= u_{,\zeta}(1 - \zeta z_{,xx}) + w_{,x} + z_{,y}v_{,x} + z_{,x}(w_{,\zeta} - u_{,x}) \\
&\quad - \zeta z_{,xy}v_{,\zeta} + u_{,x}u_{,\zeta} + v_{,x}v_{,\zeta} + w_{,x}w_{,\zeta} \\
2e_{xy} &= u_{,y}(1 - \zeta z_{,xx}) + v_{,x}(1 - \zeta z_{,yy}) + z_{,x}w_{,y} + z_{,y}w_{,x} \\
&\quad - \zeta z_{,xy}(u_{,x} + v_{,y}) + u_{,x}u_{,y} + v_{,x}v_{,y} + w_{,x}w_{,y} \quad (61)
\end{aligned}$$

It should be noted that the strain-displacement relations above do not involve the orientation of the displaced midsurface normal, and, therefore, apply to arbitrarily large displacements and rotations of the shell. The definitions of the linear and nonlinear portions of the incremental strains ( $\Delta \Sigma_{ij}$  and  $\Delta \eta_{ij}$  in Equations 18 and 19) follow directly from Equations 62<sup>11</sup>.

In order to ensure proper behavior of the finite element approximation, constraints must be applied to enforce the conditions of thin shell response. To prescribe the condition that line elements initially normal to the shell midsurface remain straight, normal to the surface and unstrained, it is necessary to suppress the virtual work due to transverse shear and normal strains, and to enforce constraint relations of the form

$$\Delta e_{x\zeta} = \Delta e_{y\zeta} = \Delta e_{\zeta\zeta} = 0. \quad (62)$$

A particularly effective method of enforcing the constraints of Equation 62 is developed in Reference 11, by defining a penalty functional which, in the limit, forces Equation 62 to be satisfied at selected discrete points within an element. Define the functional

$$\begin{aligned}
\Delta \Pi_c = & \sum_{m=1}^M \left[ \frac{1}{2} w_x \Delta e_{xz}^2(\vec{r}_m) \right. \\
& + \frac{1}{2} w_y \Delta e_{yz}^2(\vec{r}_m) \\
& \left. + \frac{1}{2} w_z \Delta e_{zz}^2(\vec{r}_m) \right] \quad (63)
\end{aligned}$$

in which  $M$  is the number of constraint locations,  $w_x, w_y, w_z$  are positive weights, and  $\vec{r}_m$  is the location at which the  $m^{\text{th}}$  constant is to be enforced. Observe that, by setting  $\delta(\Delta \Pi_c) = 0$ , Equation 62 is satisfied identically at each of the points  $\vec{r}_m$ ;  $m=1, 2, \dots, M$ .

Introducing the above constraints into the incremental principle of virtual work, Equation 21, yields

$$\begin{aligned}
\int_V [D_{\alpha\beta\lambda\mu} (\Delta e_{\lambda\mu} - \alpha_{\lambda\mu} \Delta T) \delta \Delta e_{\alpha\beta} + l_{\alpha\beta} \delta \Delta \eta_{\alpha\beta}] dV \\
- \int_{\partial V} \Delta \bar{t}_i \delta \Delta u_i dA + \delta(\Delta \Pi_c) = 0. \quad (64)
\end{aligned}$$

In Equation 64, Greek subscripts imply a range of summation of 2, while Latin indices have a range of 3. The additional thin shell constraint of vanishing normal stress through the thickness ( $\sigma_{zz} = 0$ ) is enforced exactly in Equation 64. Thus, the stress-strain relation for the remaining nonzero stresses and strains is one of plane stress.

To cast Equation 64 in matrix form, the following quantities are defined. Let

$$\vec{u}^T = [\Delta u \quad \Delta v \quad \Delta w] \quad (65)$$

$$\vec{F}^T = [\Delta u_{,x} \quad \Delta u_{,y} \quad \Delta u_{,z} \quad \Delta v_{,x} \quad \Delta v_{,y} \quad \Delta v_{,z} \quad \Delta w_{,x} \quad \Delta w_{,y} \quad \Delta w_{,z}] \quad (66)$$

$$\vec{e}^T = [\Delta e_{xx} \quad \Delta e_{yy} \quad 2\Delta e_{xy}] \quad (67)$$

$$\underline{\gamma}^T = [\Delta e_{xz} \quad \Delta e_{yz} \quad \Delta e_{zz}] \quad (68)$$

$$\underline{\sigma}^T = [\sigma_{xx} \quad \sigma_{yy} \quad \sigma_{xy}] \quad (69)$$

$$\underline{\tau} = \begin{bmatrix} \sigma_{xx} & \sigma_{xy} & 0 \\ \sigma_{xy} & \sigma_{yy} & 0 \\ 0 & 0 & 0 \end{bmatrix} \quad (70)$$

$$\underline{\tau}^* = \begin{bmatrix} \underline{\tau} & 0 & 0 \\ 0 & \underline{\tau} & 0 \\ 0 & 0 & \underline{\tau} \end{bmatrix} \quad (71)$$

$$\underline{\alpha}^T = [\alpha \quad \alpha \quad \alpha] \quad (72)$$

$$\underline{W} = \begin{bmatrix} W_x & 0 & 0 \\ 0 & W_y & 0 \\ 0 & 0 & W_z \end{bmatrix} \quad (73)$$

$$\underline{\tau}^T = [\Delta \tau_x \quad \Delta \tau_y \quad \Delta \tau_z] \quad (74)$$

The constrained principle of virtual work then becomes

$$\begin{aligned} & \int_V [\delta \underline{e}^T D (\underline{e} - \underline{\alpha} \Delta T) + \delta \underline{F}^T \underline{\tau}^* \underline{F}] dV \\ & + \sum_{m=1}^M \delta \underline{\gamma}^T(\vec{r}_m) \underline{W} \underline{\gamma}(\vec{r}_m) = \int_{\partial V} \delta u^T \underline{\tau} dA, \end{aligned} \quad (75)$$

which is the basis of the thin shell finite element. It remains only to specify an appropriate approximation for  $\underline{u}$  in terms of a finite number of unknown parameters.

In selecting the finite element approximation for  $u$  in Equation 75, it is noted that only first-order derivatives of the displacement appear in the energy form of the equations. Thus, any approximation which preserves continuity of displacements (but which may violate the continuity of slopes between elements) is admissible. For the present development the simplest possible forms, piecewise linear polynomials, are selected. Defining the natural coordinates  $\xi_i; i=1,2,3$  which vary between -1 and 1 within an element, the appropriate one-dimensional functions are

$$\begin{aligned} L_1(\xi) &= \frac{1}{2}(1 - \xi) \\ L_2(\xi) &= \frac{1}{2}(1 + \xi). \end{aligned} \quad (76)$$

Letting

$$\begin{aligned} N_1(\xi) &= L_1(\xi_1) L_1(\xi_2) L_1(\xi_3) \\ N_2(\xi) &= L_2(\xi_1) L_1(\xi_2) L_1(\xi_3) \\ N_3(\xi) &= L_2(\xi_1) L_2(\xi_2) L_1(\xi_3) \\ N_4(\xi) &= L_1(\xi_1) L_2(\xi_2) L_1(\xi_3) \\ N_5(\xi) &= L_1(\xi_1) L_1(\xi_2) L_2(\xi_3) \\ N_6(\xi) &= L_2(\xi_1) L_1(\xi_2) L_2(\xi_3) \\ N_7(\xi) &= L_2(\xi_1) L_2(\xi_2) L_2(\xi_3) \\ N_8(\xi) &= L_1(\xi_1) L_2(\xi_2) L_2(\xi_3) \end{aligned} \quad (77)$$

the form of the approximate displacement field within a single element is

$$U(\xi) = \sum_{i=1}^8 N_i(\xi) U_i = \tilde{N}^T \tilde{U}. \quad (78)$$

Here  $U_i$ ;  $i, 2, \dots, 8$  are values of the displacement  $u$  at the eight nodal points of an element, as shown in Figure 3. The displacements  $u, w$  are represented in exactly the same manner.

Substitution of the above approximation into Equation 75 leads to the definition of the tangent stiffness matrix  $\tilde{K}_T$ , the geometric stiffness  $\tilde{K}_G$ , a discrete "constraint stiffness"  $\tilde{K}_C$ , and the external force vector  $\tilde{T}$ . In matrix form, the equilibrium relation for a single element becomes

$$(\tilde{K}_T + \tilde{K}_G + \tilde{K}_C) \tilde{U} = \tilde{T} \quad (79)$$

which can be solved iteratively as shown in Section 4.

### 3.2 SANDWICH CORE ELEMENTS

The sandwich core finite elements employed in the present work are obtained directly from the three-dimensional nonlinear formulation of Section 2, without any specialization. Orthotropic stress-strain relations, as described in Paragraph 2.2, are permitted for analyzing orthotropic cores (e.g., metal honeycomb core), and to represent the very low extensional moduli typical of many types of core. Permanent deformations, such as core crushing, can be treated in an approximate fashion using the elastic-plastic material law described in Paragraph 2.3.

The core element is shown in Figure 4. In the planform directions, a linear interpolation of the displacements is used for compatibility with the face sheet element (Paragraph 3.1). Linear displacement shape functions are also employed through the core thickness; due to the typical high flexibility of the core layers in transverse shear, linear displacements are nearly always an adequate approximation. Due to the very simple nature of the displacement state approximation, the resulting element

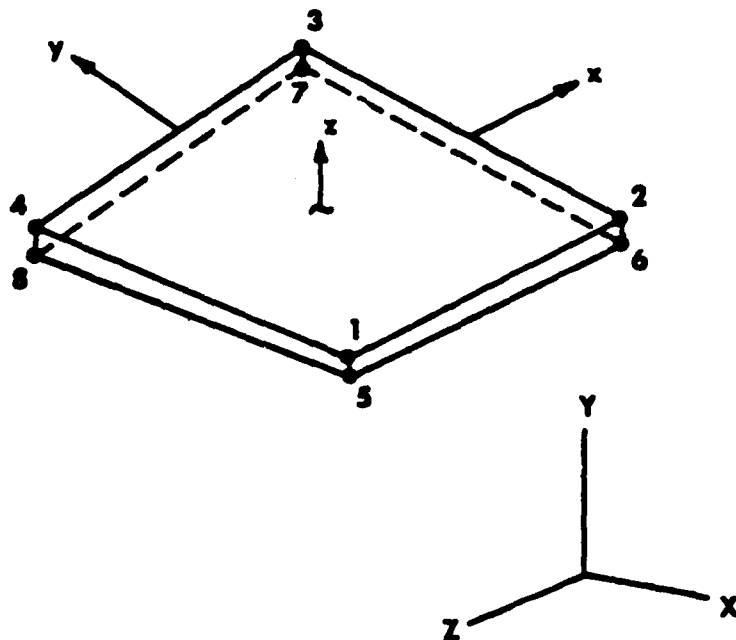


Figure 3. Thin Shell and Sandwich Face Sheet Element.

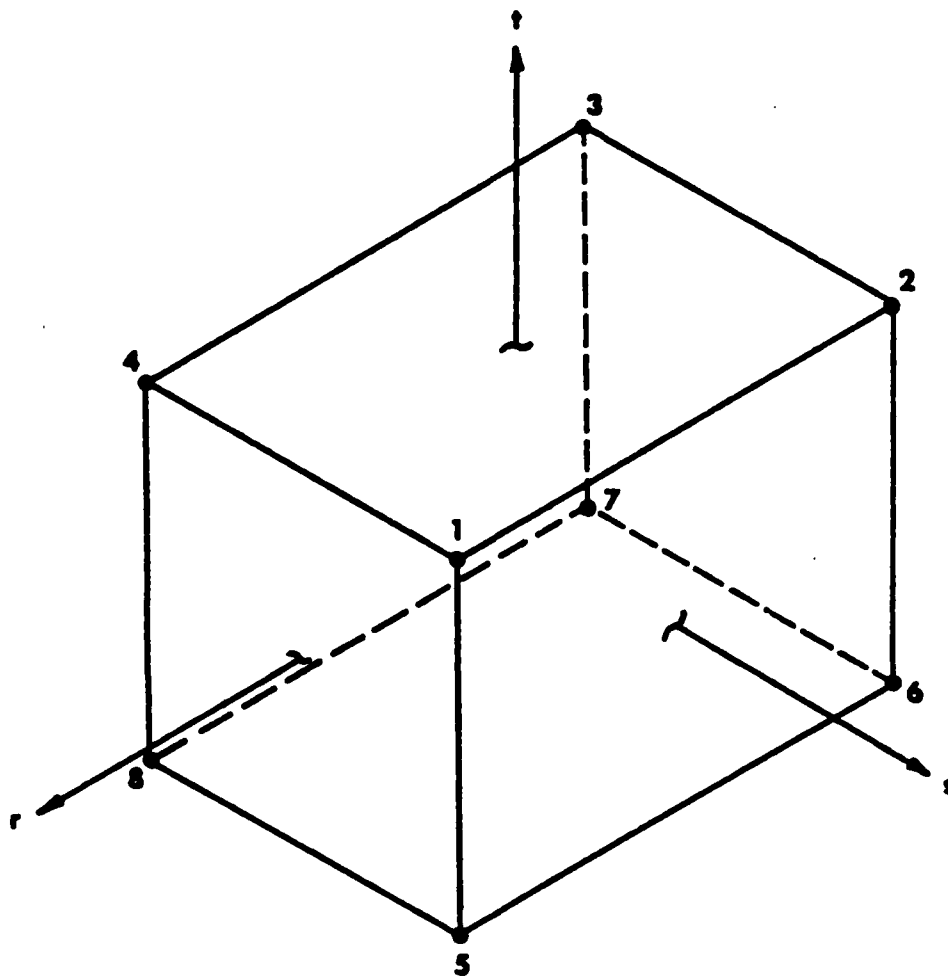


Figure 4. Sandwich Core Finite Element.

may become excessively "stiff" when integrated exactly<sup>11</sup>. For this reason, a single integration point is used in each core element to provide improved accuracy with this simple approximation. Although the core element alone would prove to be unstable using the single point integration rule, the addition of face sheet and closeout elements provides a stabilizing effect which eliminates singularity in the final system of equations. When stabilized in this manner, the simple core element used here provides a highly effective and accurate representation of the sandwich response.

### 3.3 STIFFENING MEMBERS

Beam stiffener elements obtained here from the general formulation of Section 2 are of two types: face sheet stiffeners and full-depth stiffeners. The face sheet stiffening member is used to represent discrete beam stiffeners attached to the inner or outer surface of a sandwich panel. The full-depth stiffener is used to model spar panels connected to both the upper and lower face sheets of a sandwich, or to represent panel edge closeouts. Both of these configurations are shown in Figure 5.

Stiffener elements of both types have similar geometry, shown in Figure 6. The coordinates  $X_L$ ,  $Y_L$  are local coordinates, embedded in the plane of an element. In this local coordinate system, the transverse stresses  $\sigma_{xz}$ ,  $\sigma_{yz}$  and  $\sigma_{zz}$  are assumed to vanish, and thus the stress-strain relation for an element has the form appropriate for a plane state of stress. The resulting element models extension, primary bending, and twisting effects. Again, compatibility is achieved with the other sandwich elements through the use of linear displacement shape functions. To avoid excessive stiffness of the element in bending, a selective integration<sup>11</sup> scheme is used for the in-plane shear strain energy.

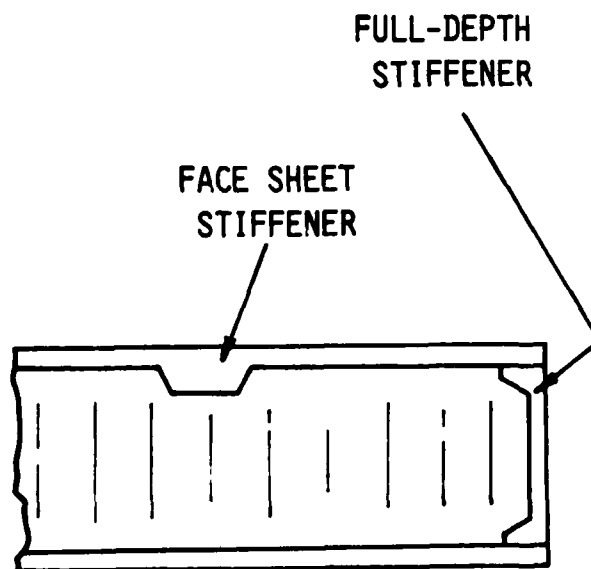


**Figure 5. Face Sheet Stiffener and Full-Depth Stiffener Element Configurations.**

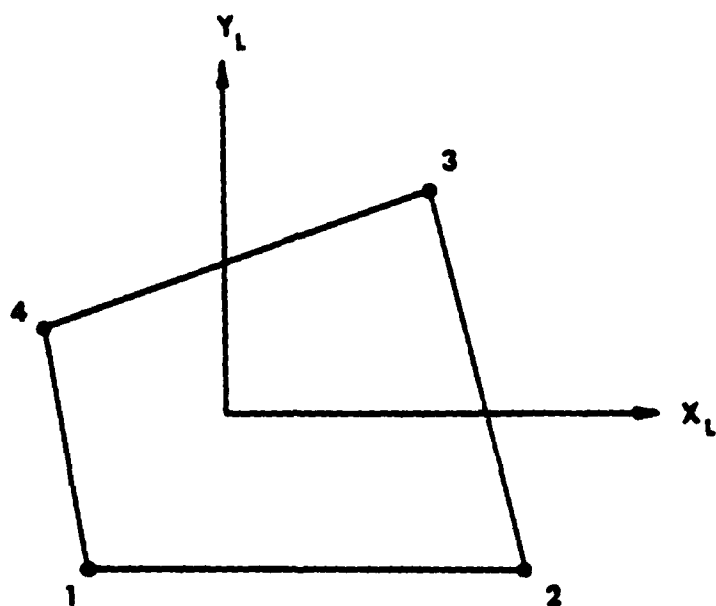


Figure 6. Stiffener Element Geometry.

### 3.4 THREE-DIMENSIONAL SOLID ELEMENTS

A three-dimensional continuum finite element is included in the present formulation, for use in the modeling of:

- general structural configurations,
- transitions between sandwich panels and surrounding components, and
- detailed aspects of the deformation of sandwich panels.

The element, which has a variable number of nodes, can be made compatible with the sandwich face sheet and/or core elements (which use linear shape functions) on selected element surfaces while higher-order displacement functions are used elsewhere in the element. Thus, transitions from sandwich panels to attachments or other supporting structure can be represented quite simply. Since the solid element is fully three-dimensional, it is also useful for detailed analysis of effects such as core crushing or plastic deformation of the sandwich face sheets.

The general solid element is pictured in Figure 7. Node points 1 through 8 (the vertices) are required for each element; however, each of the remaining 12 midside nodes may be included or deleted as required. In most instances, the use of the midside nodes is highly desirable in terms of accuracy. The solid element may be numerically integrated using either an eight-point (2x2x2) or 27-point (3x3x3) Gaussian quadrature formula.

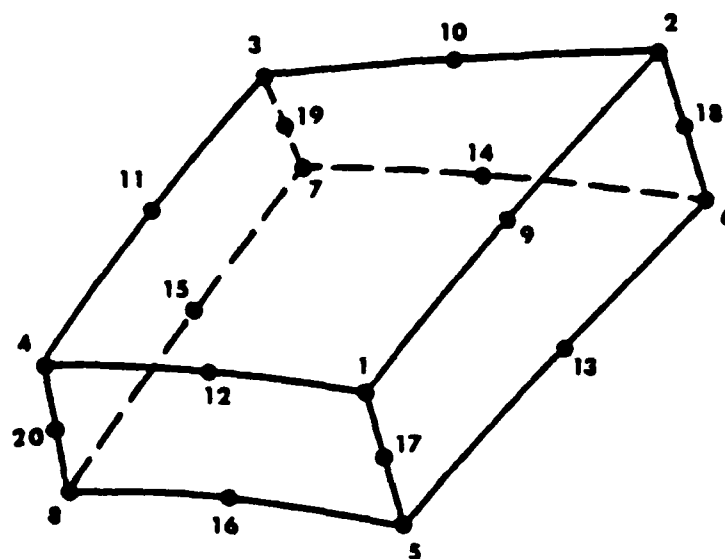


Figure 7. Three-Dimensional Solid Element.

## SECTION 4

### NUMERICAL SOLUTION TECHNIQUES

In this section, the methodology used in solving the governing equations for a complete assemblage of finite elements is described. Static response may be computed with or without nonlinear effects included, and considering both thermal and mechanical loadings. The option to compute a specified number of natural vibration frequencies and their associated mode shapes is also provided.

#### 4.1 STATIC RESPONSE SOLUTION

In static problems, the finite element equations take the form

$$(\underline{K}_T + \underline{K}_G)\underline{\Delta U} = \underline{\Delta T} \quad (80)$$

in which

- $\underline{K}_T$  = tangent stiffness matrix,
- $\underline{K}_G$  = geometric (initial stress) stiffness,
- $\underline{\Delta U}$  = incremental nodal displacements, and
- $\underline{\Delta T}$  = incremental nodal forces, including both mechanical and thermal effects.

The tangent stiffness, for nonlinear problems, is a function of the total displacements,  $\underline{K}_T + \underline{K}_T(\underline{U})$ , and the geometric stiffness depends upon the current stress level,  $\underline{K}_G = \underline{K}_G(\underline{\sigma})$ .

When the problem is assumed to be linear (small displacements, elastic material behavior),  $\underline{K}_T = \underline{K}_E$ , the linear stiffness, and  $\underline{K}_G = \underline{0}$ . In this case, Equation 80 can be written using the total displacements  $\underline{U}$  and forces  $\underline{T}$ :

$$\underline{K}_E \underline{U} = \underline{T}. \quad (81)$$

A direct solution is obtained by factoring  $K_E$  as

$$\underline{K}_E = \underline{L} \underline{D} \underline{L}^T \quad (82)$$

where  $\underline{L}$  is a unit lower triangular matrix and  $\underline{D}$  is diagonal. Next letting

$$\underline{Z} = \underline{D} \underline{L}^T \underline{U}, \quad (83)$$

the relation

$$\underline{L} \underline{Z} = \underline{T} \quad (84)$$

can be solved directly for  $\underline{Z}$ . Similarly, Equation 83 gives

$$\underline{L}^T \underline{U} = \underline{D}^{-1} \underline{Z} \quad (85)$$

which can finally be solved for  $\underline{U}$ . Knowing the displacement solution, strain and stress information can be computed at selected locations in the model to complete the linear analysis.

When nonlinear effects are considered in the solution of Equation 80, an iterative technique must be adopted. In addition, the nonlinear solution is usually performed in an incremental fashion, by applying the total loading in a number of steps. Such an approach is adopted to provide the static solution for an entire range of loading, to enhance convergence, and to facilitate the detection of buckling or similar phenomena. In plastic analysis, this incremental method is necessary due to the history-dependent nature of the response.

The nonlinear equations are solved using various forms of the Newton-Raphson method, as shown in Figure 8. First, the nonlinear system is written as

$$(\underline{K}_T + \underline{K}_G) \Delta \underline{U} = \underline{T} - \underline{I} \quad (86)$$

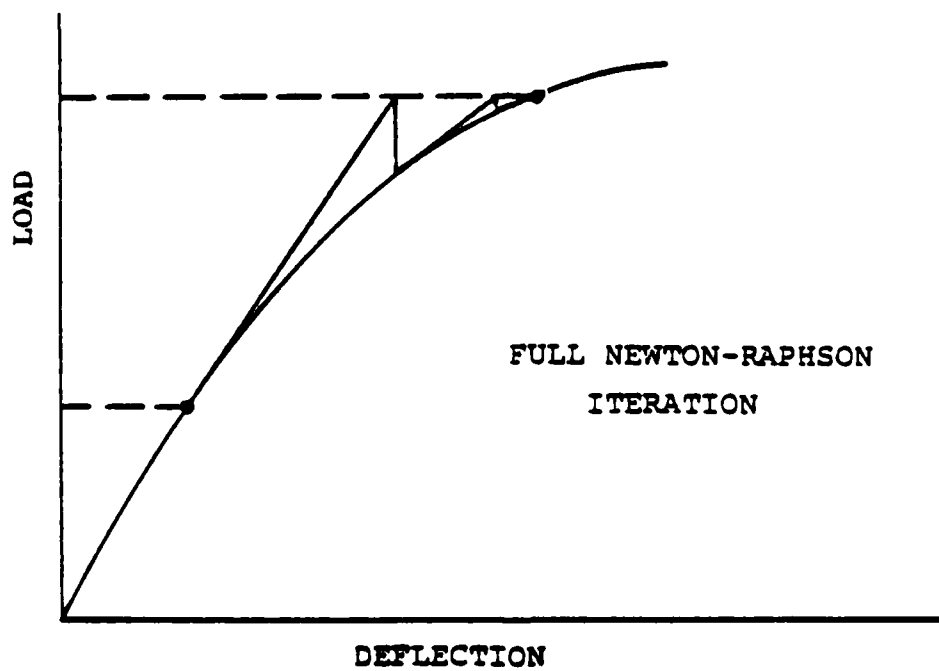
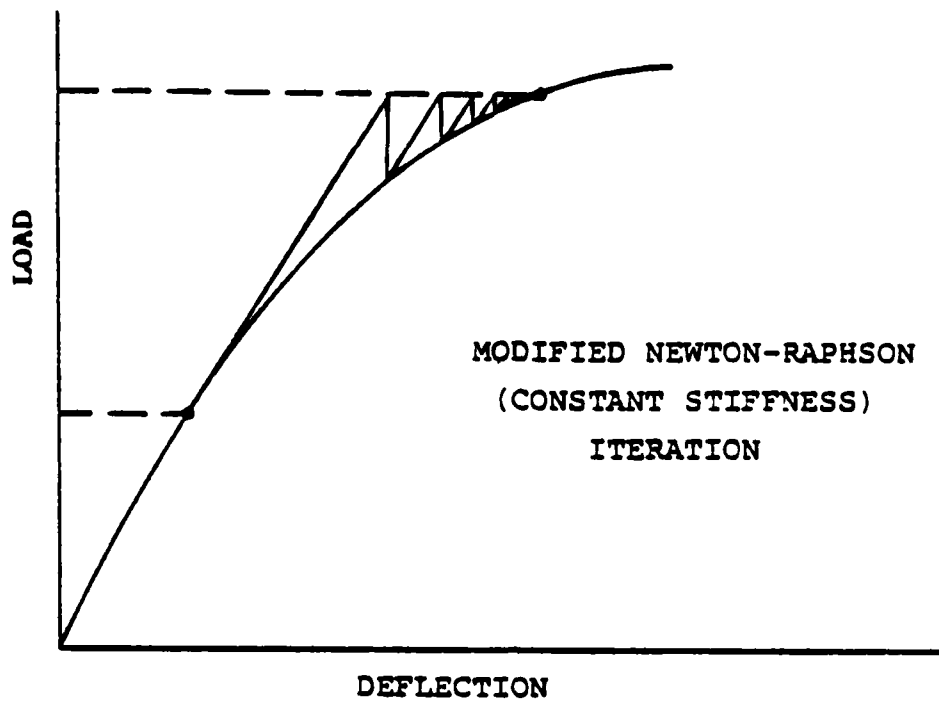


Figure 8. Newton-Raphson Method for the Solution of Nonlinear Equations.

where  $\underline{T}$  is the total applied loading and  $\underline{I}$  are the internal forces based upon the current (computed) state of stress. Once the computed stress state is in equilibrium with the external loading, the right-hand side of Equation 86 becomes zero. Thus, Equation 86 can be used repeatedly to compute corrections to an estimated displacement state for given  $\underline{T}$ , until the equilibrium condition ( $\underline{T} = \underline{I}$ ) is satisfied to within a specified tolerance. During a full Newton-Raphson solution, the coefficient matrix is updated at each iteration cycle. In the modified Newton solution, the stiffness matrix is reformed only at the start of an increment, as indicated in Figure 8. The conventional Newton's method tends to converge rapidly, with each iteration consuming a relatively large amount of processor time; with the modified iteration, each cycle of iteration is computationally simpler, but convergence is generally rather slow.

#### 4.2 NATURAL FREQUENCY SOLUTION

When free vibrations are considered, the problem is assumed to be linear, and the forcing function  $\underline{T}$  is replaced by the inertial forces,

$$\underline{K}_E \underline{U} = -\underline{M} \ddot{\underline{U}} \quad (87)$$

where  $\underline{M}$  is the structure mass matrix. For harmonic motions, then, the nodal displacements are

$$\underline{U} = \underline{X} \sin \omega t \quad (88)$$

and the equation of motion becomes

$$\underline{K}_E \underline{X} = \omega^2 \underline{M} \underline{X}. \quad (89)$$

Notice that the vector  $\underline{X}$  describes only the relative displacements of the node points, and represents a mode shape corresponding to the circular frequency of vibration,  $\omega$ . If  $\underline{K}_E$  and  $\underline{M}$  are matrices

of order  $N$ , then there exist  $N$ -solutions of Equation 89:  $\omega_i$ ,  $X_i$ ;  $i=1,2,\dots,N$ .

Generally only the lowest few frequencies and mode shapes of the system will be of interest, and, therefore, a vector iteration procedure is most appropriate. In the present development, the method of simultaneous vector iteration<sup>13</sup> is used.

If  $K_E$  can be expressed in the Choleski-factored form

$$K_E = LL^T \quad (90)$$

with  $L$  a lower triangular matrix, then the transformation

$$Y = L^T X \quad (91)$$

allows Equation 89 to be written in the standard form

$$AY = \frac{1}{\omega^2} Y. \quad (92)$$

Here  $A$  is defined by

$$A = L^{-1}ML^{-T}. \quad (93)$$

Given a set of trial solution vectors  $Y_i$ ;  $i=1,2,\dots,m$ , a partial modal matrix is formed,

$$\Phi = [Y_1 \ Y_2 \ \cdot \ \cdot \ \cdot \ Y_m]. \quad (94)$$

Noting that any set of eigenvectors of  $A$  must be orthogonal with respect to  $A$ , the next step is to inspect the "interaction matrix"

$$B = \Phi^T A \Phi \quad (95)$$

which is diagonal if the columns of  $\phi$  are true eigenvectors. When the vectors  $\underline{y}_i$  are properly normalized, the diagonal entries of  $\underline{B}$  are estimates of the eigenvalues

$$\omega_i = \sqrt{b_{ii}} \quad (96)$$

Before the solution has converged, the interaction matrix  $\underline{B}$  is not diagonal. Instead, an approximate solution can be performed for  $\underline{B}$  to obtain an improved estimate of the eigenvalues. The trial vectors (i.e., columns of  $\phi$ ) are then modified accordingly, orthogonalized, and used in the next iteration cycle.

A solution for the lowest several frequencies and mode shapes using simultaneous iteration tends to converge in very few iterations, provided the number of trial iteration vectors is sufficient. If  $p$  is the number of natural frequencies to be solved, an estimate for the proper number of trial vectors can be obtained from

$$m = \min[2p, p + 5]. \quad (97)$$

The procedure in general tends to be quite fast, since only one factorization of  $\underline{K}_E$  is required, and can be performed economically without actually forming the matrix  $\underline{A}$  (Equation 92).

## SECTION 5

### SAMPLE ANALYSES

Several sample problems are presented in this Section to demonstrate the analytical capabilities of the present finite element formulation. Classes of problems considered include large deflection and elastic-plastic analysis, buckling, natural frequency solutions and thermal stress analysis.

#### 5.1 NONLINEAR ANALYSIS OF A SANDWICH PANEL UNDER PRESSURE

A square sandwich panel, 50 inches on each side, is subjected to a uniform lateral pressure. The three-layer plate, shown in Figure 9, has identical aluminum face sheets ( $E = 10.5 \times 10^6$  psi;  $\nu = 0.3$ ) 0.015 inches thick, bonded to an aluminum honeycomb core of one inch thick. The core is assumed to be isotropic, with shear modulus  $G = 50,000$  psi. All boundaries of the sandwich are fully clamped.

Due to symmetry of the geometry and loading, one quarter of the panel is considered in the finite element solution. The finite element discretization consists of a total of 75 finite elements, 25 in each layer. The two face sheets are modeled using eight-node, thin shell elements (Paragraph 3.1). Three-dimensional sandwich core elements (Paragraph 3.2) are used for the central layer. Note that these element types are fully compatible so that no special constraints are necessary for joining the individual layers. The nonlinear solution has been obtained in load increments of one psi to a total pressure of 20 psi followed by two psi increments to 30 psi.

The nonlinear central displacement of the sandwich is plotted versus load in Figure 10. Nonlinear finite element results obtained by Monforton<sup>2</sup>, using 16 specially formulated bicubic sandwich elements, are shown for comparison. Agreement between the two finite element solutions is quite good. Figure 10 also shows the perturbation solution of Kan and Huang<sup>14</sup>, given by

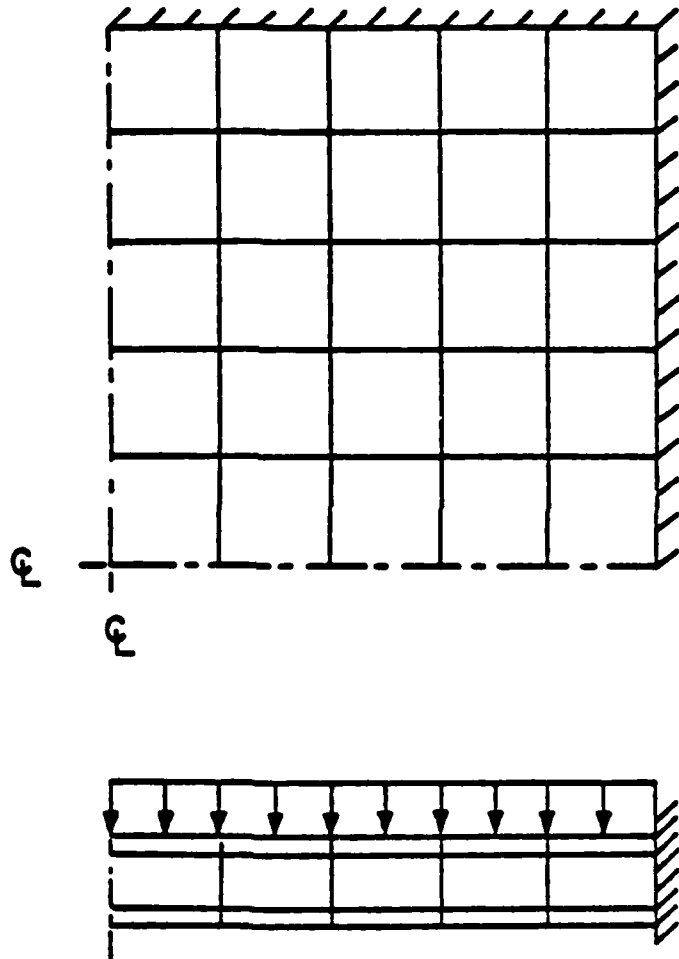


Figure 9. Sandwich Panel Under Uniform Lateral Pressure.

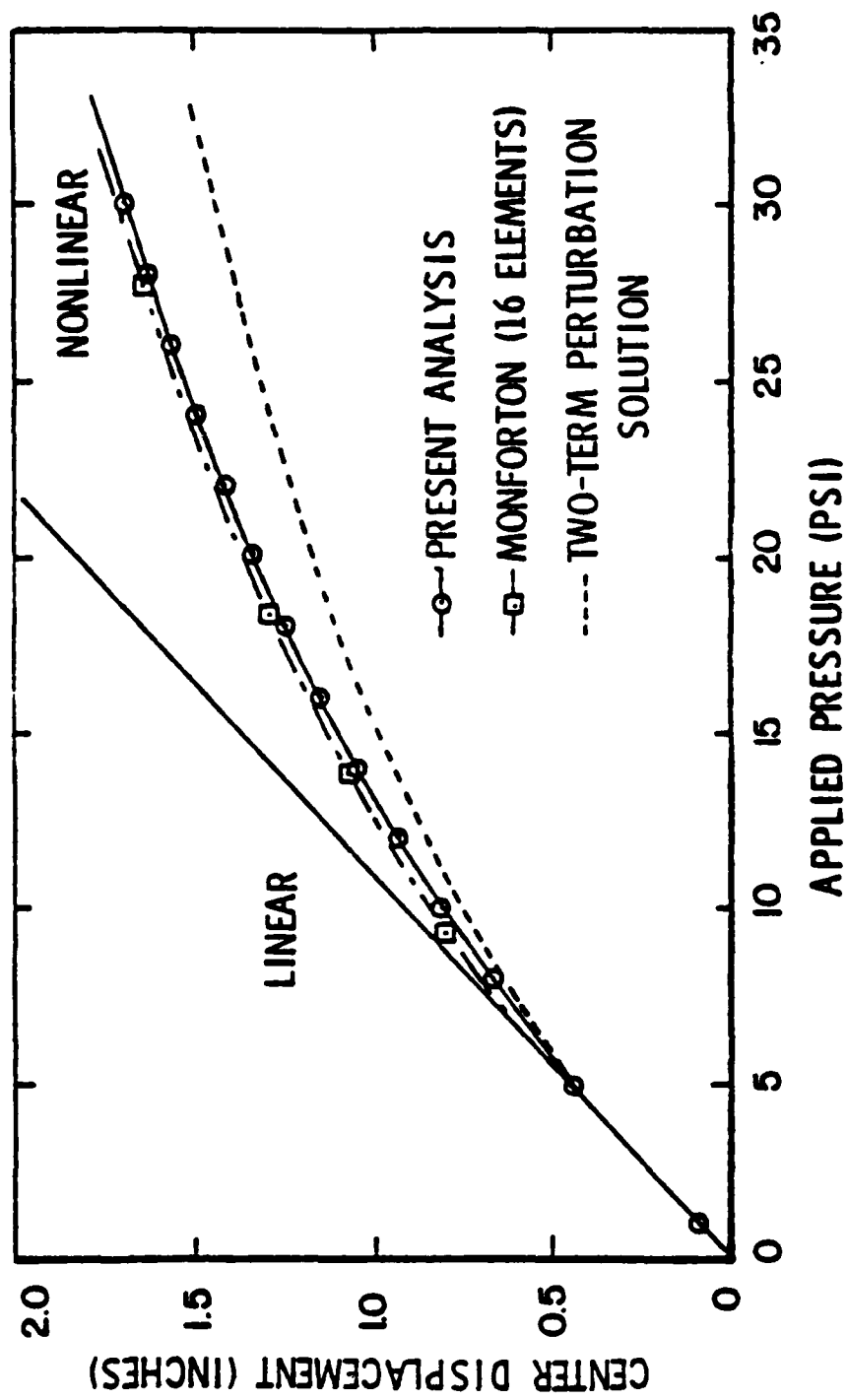


Figure 10. Load-versus-Deflection Curve for Uniformly Loaded Panel.

$$q = 10.5299w_c + 4.8550w_c^3 \quad (98)$$

in which  $q$  is the applied pressure and  $w_c$  the transverse center displacement. The analytical solution of Reference 14 is valid for deflections which are smaller than the core thickness, and reasonable agreement with the two numerical solutions is observed in this region. For larger deflections, the perturbation analysis requires more terms for acceptable accuracy; the two-term solution gives results which overestimate the influence of membrane stiffening upon the panel deflection.

## 5.2 NATURAL FREQUENCIES OF SANDWICH PANELS WITH VARIOUS BOUNDARY CONDITIONS

The three-layer sandwich plate shown in Figure 11 has been analyzed for its free vibration response using a number of different edge conditions. The finite element model of the panel consists of 36 elements in each layer, and contains a total of 196 nodes and 480 unconstrained degrees of freedom. Material properties and dimensions of the specimen are as follows:

Dimensions :  $a = 62.25$  in.  
 $b = 43.50$  in.  
 $t_f = 0.072$  in.  
 $t_c = 1.856$  in.  
 Face Sheets:  $E = 1.0 \times 10^7$  psi  
 $\nu = 0.33$   
 Core Layer :  $G_{xz} = 30000$ . psi  
 $G_{yz} = 30000$ . psi  
 $E_z = 60000$ . psi

Three types of edge conditions have been considered in the present analysis. The first is a simply-supported condition in which in-plane motions of the edge are permitted; this type of constraint allows a pure-bending type of response of the entire panel and is readily verified with known analytical solutions.

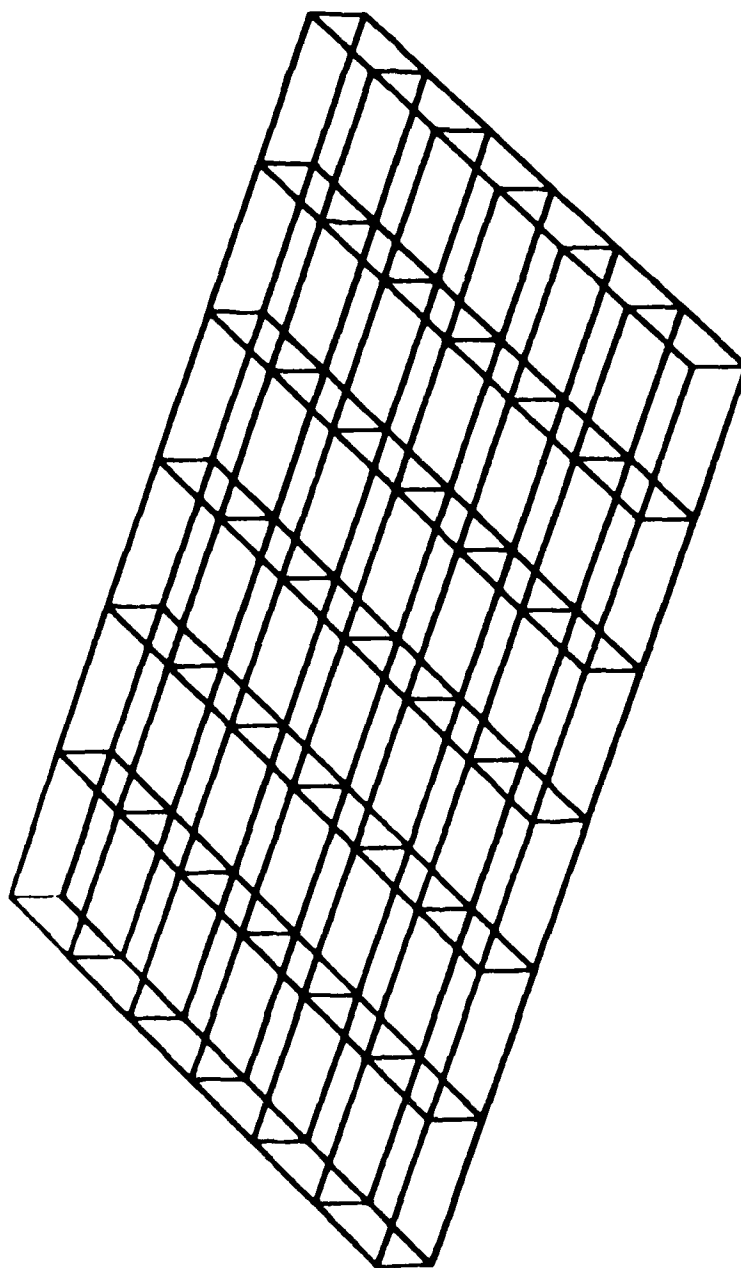


Figure 11. Three-Layer Sandwich Panel used in Natural Frequency Calculations.

For the second type of constraint, in-plane displacements are prevented on the lower face of the panel, introducing a net stretching effect when transverse bending occurs. The third boundary condition used is a fully clamped edge.

Fundamental frequencies of these panels are summarized in Table 1. For the first set of edge conditions, analytical frequencies computed from the formulation of Reference 15 are also listed. Agreement between the two solutions is good. The stiffening effect produced by the two alternative boundary conditions is clearly shown in the frequency results.

### 5.3 BUCKLING OF A SIMPLY-SUPPORTED SANDWICH PLATE

The compressive buckling of a plate of sandwich construction is considered. A square, three-layer panel (Figure 12) is subjected to a uniform compressive load of  $\bar{N}_x$  pounds per inch. The panel is 23.5 inches on each side, and supported at each face of the sandwich on all four edges (vertical displacements only are prevented).

The outer face sheets of the panel, which are represented by thin shell finite elements, are each 0.021 inches in thickness, with isotropic material properties  $E = 9.5 \times 10^6$  psi,  $\nu = 0.3$ . The core layer, 0.181 inches thick, has a transverse shear rigidity  $G = 19000$  psi. Each layer of the model contains 16 elements of equal planform dimensions. Only one quadrant of the panel is considered in the numerical solution, due to symmetry of the geometry and loading. On the lateral boundaries, the tangential transverse shear strains within the core are suppressed by making the upper and lower face sheet displacements equal in the direction parallel to each edge.

A solution for the buckling load  $\bar{N}_{CR}$  has been obtained by applying the in-plane forces incrementally until a sudden increase in transverse displacement is observed. Out of plane deflections are triggered by a small (one pound) transverse load applied at the center of the plate. Buckling is found to

TABLE 1  
NATURAL FREQUENCY RESULTS FOR FLAT SANDWICH PANEL  
WITH VARIOUS BOUNDARY CONDITIONS

Boundary Condition	Frequency, Hz (Computed)	Frequency, Hz (Analytical)
Simple Support Inplane Motion Permitted	174	170
Simple Support No Inplane Motion	211	-
Clamped Edge	288	-

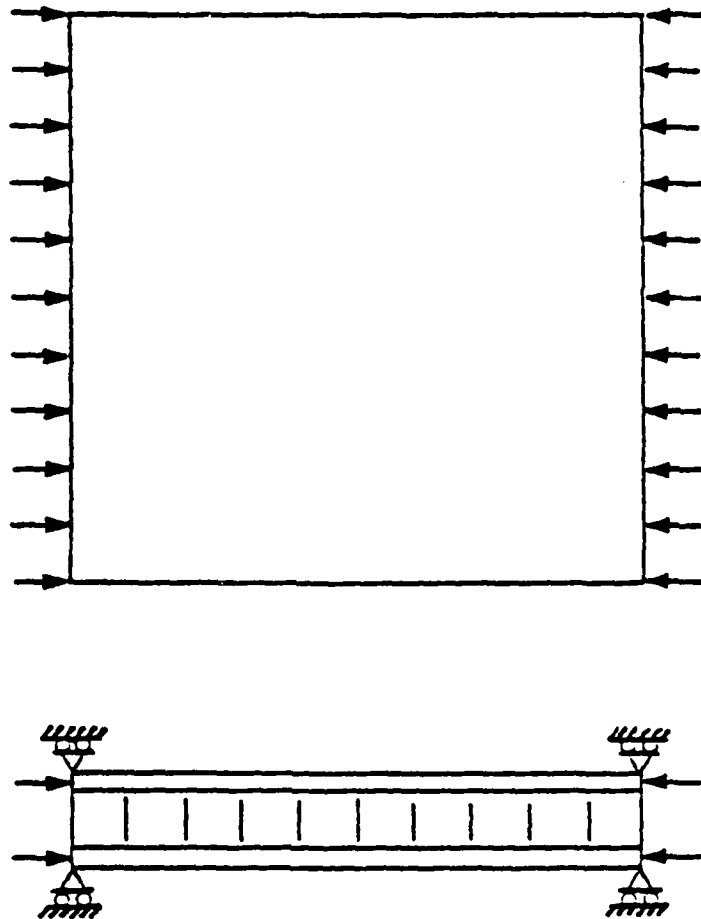


Figure 12. Simply Supported Sandwich Panel Under Edge Compression.

occur for an applied load of  $\bar{N}_x = 305$  pounds per inch; this computed value compares well with previous analytical and experimental results, as shown in Table 2. It is noted that all of the analytical results give estimates of the critical load which are about nine percent too high; it is likely that the assumption of zero transverse shear strains at the panel boundaries is largely responsible for this error. The transverse shear constraint has been used in the present finite element solution to permit comparison with previous analytical solutions.

#### 5.4 PLASTIC ANALYSIS OF A TOROIDAL SANDWICH SHELL

A toroidal sandwich shell panel under line loading has been analyzed to determine its elastic-plastic response. The following geometric parameters are used:

major radius	$R = 5.0$ inches
included angle	$\theta_R = 75.0$ degrees
minor radius	$r = 1.5$ inches
included angle	$\theta_r = 90.0$ degrees
core thickness	$t_c = 0.90$ inches
face thickness	$t_f = 0.05$ inches

The geometry of the shell is shown (in the form of a finite element model) in Figure 13. Figure 14 shows the outer face sheet of the sandwich with node numbers on the exterior surface labeled. A line load is applied in the vertical direction along the upper edge of the shell (nodes 36, 56, 92, ..., 316 in Figure 14). The two short edges of the panel are fully clamped.

The panel is constructed of aluminum, with the properties

$$E_f = 1.0 \times 10^7 \text{ lb/in}^2$$

$$\nu_f = 0.30$$

$$G_c = 30000. \text{ lb/in}^2$$

A yield stress of  $10000 \text{ lb/in}^2$  is assumed in all layers, and the material is considered to be elastic, perfectly plastic.

TABLE 2  
COMPARISON OF BUCKLING LOADS FOR SIMPLY-SUPPORTED SANDWICH PANEL

Reference	Method	$N_{cr}$ (pounds/inch)
Hoff <sup>16</sup>	Series Solution	303.0
Plantema <sup>15</sup>	Series Solution	308.0
Brockman <sup>17</sup>	Series Solution	309.0
Boller <sup>18</sup>	Experimental	266. - 300.
Monforton <sup>2</sup>	Finite Element	307.5
Present Analysis	Finite Element	305.0

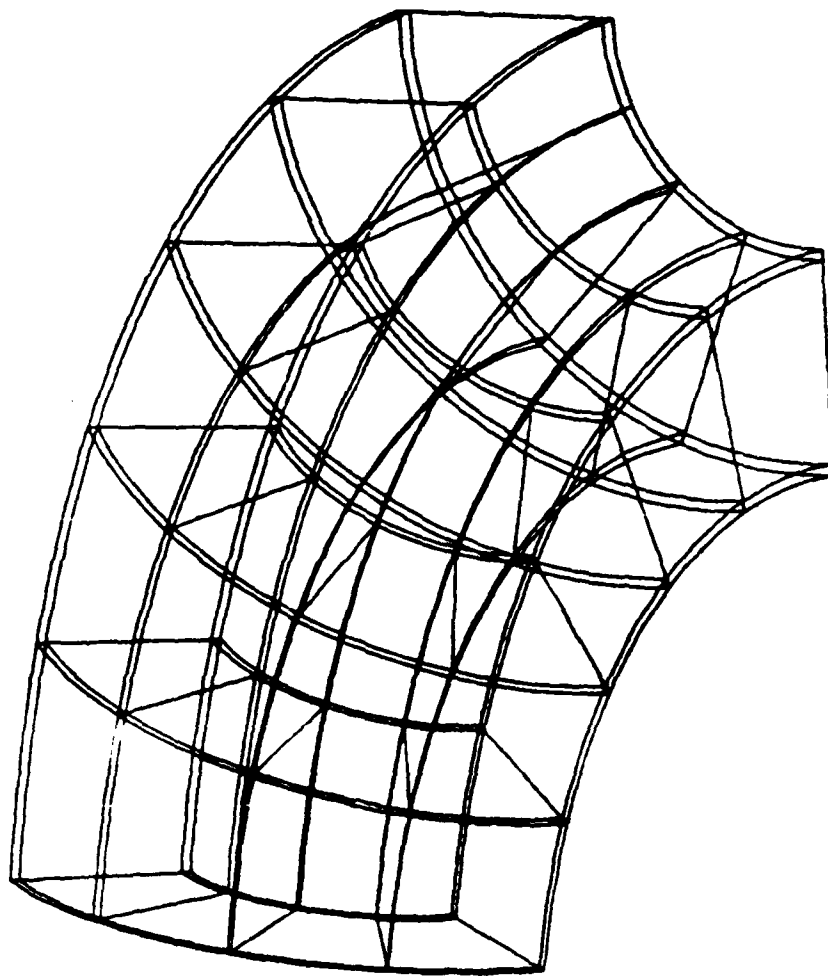


Figure 13. Toroidal Sandwich Shell.

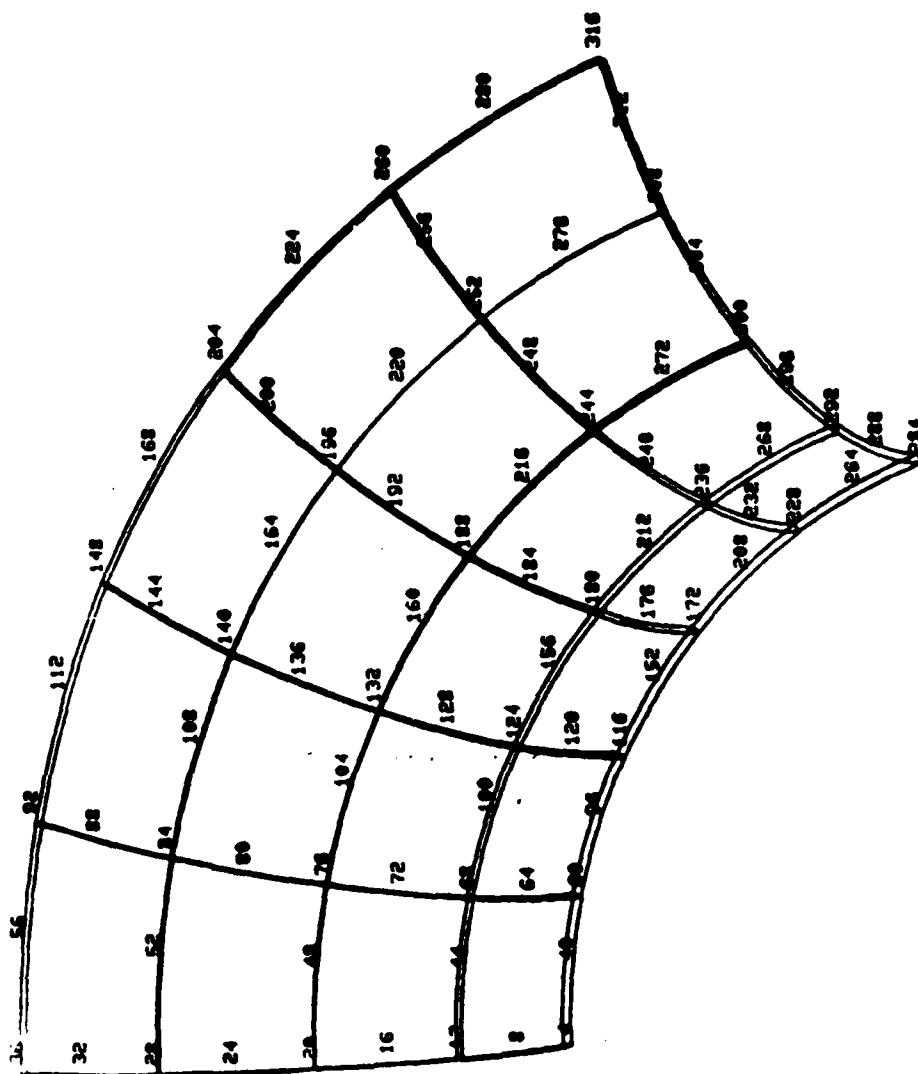


Figure 14. Upper Face Sheet of Toroidal Shell Panel with Node Numbers.

From an elastic analysis of the shell, the yield stress is found to occur at a total load of approximately 600 pounds. The elastic-plastic solution is then performed using a single increment of 600 pounds, followed by equal increments of 180 pounds to a maximum loading of 1500 pounds. Full Newton-Raphson iterations are used at each step of the solution to maintain equilibrium of the nonlinear system.

The transverse displacement at the center of the loaded edge (node 168 in Figure 14) is tabulated as a function of the total load in Table 3. Deflected shapes of the inner and outer face sheet layers are also given in Figures 15 and 16, respectively, for the maximum value of loading. Although the nonlinearity in central displacement at this loading level are rather mild (see Table 3), material yielding is extensive near the clamped edges and the loaded free boundary. Figure 17 shows the zone of plastic behavior in the outer face sheet at the maximum loading level.

#### 5.5 THERMAL STRESS ANALYSIS OF A VARIABLE-THICKNESS SANDWICH STRIP

A narrow sandwich strip with a small geometric asymmetry is subjected to uniform heating, to study the effect of the asymmetry in producing transverse deflections at high temperature. One quarter of the symmetric panel is shown in Figure 18. The uniform middle segment of the strip is 16 inches in length, while the tapered sections and ends are each two inches long. The lower face sheet is 0.075 inches in thickness. At the small ends, the thicknesses of the remaining layers are  $t_c = 0.25$  inches,  $t_f = 0.050$  inches, increasing to  $t_c = 0.50$  inches,  $t_f = 0.075$  inches in the central section. Full-depth stiffeners 0.015 in width are used to close out the lateral boundaries of the strip.

The entire strip is constructed from aluminum, the properties being

TABLE 3

LOAD-DEFLECTION HISTORY AT CENTRAL POINT ON  
LOADED EDGE OF TOROIDAL SANDWICH PANEL

<u>Increment</u>	<u>Total Load (Pounds)</u>	<u>Deflection (Node 168)</u>
-	0.	0.
1	600.	-0.00864
2	780.	-0.01141
3	960.	-0.01437
4	1140.	-0.01770
5	1320.	-0.02184
6	1500.	-0.02698

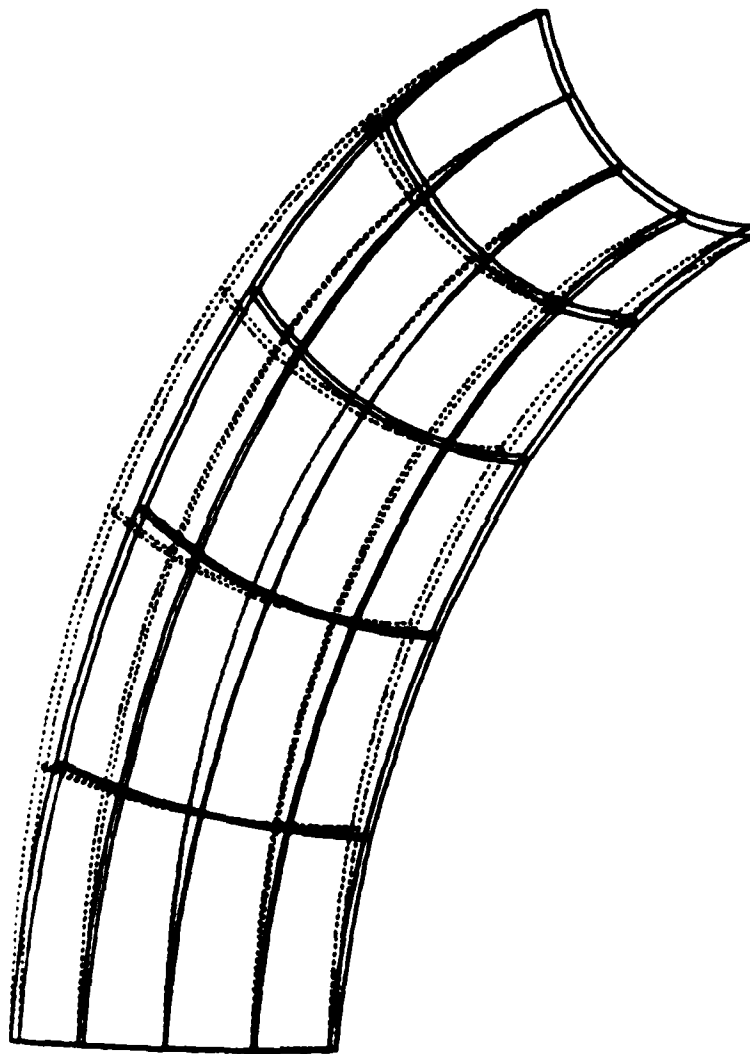


Figure 15. Deformed Shape of Inner Face Sheet at Maximum Loading.

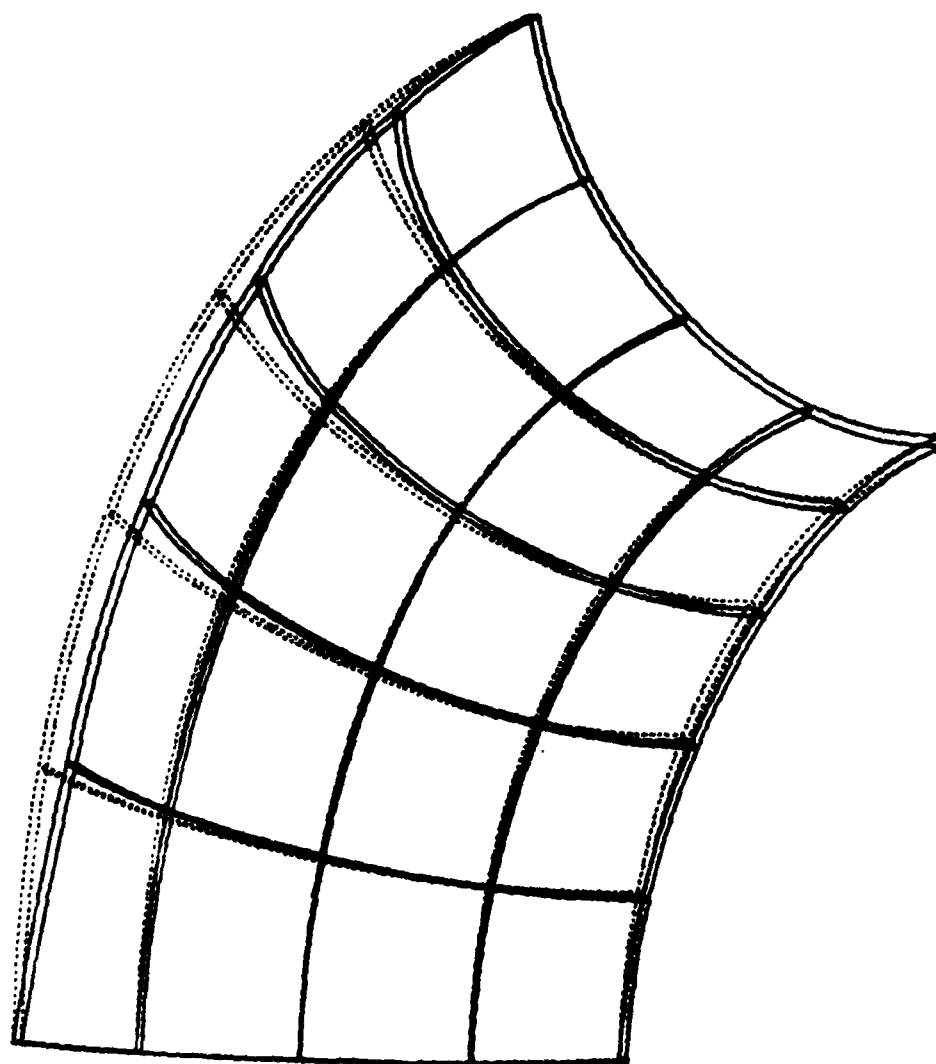


Figure 16. Deformed Shape of Outer Face Sheet at Maximum Loading.

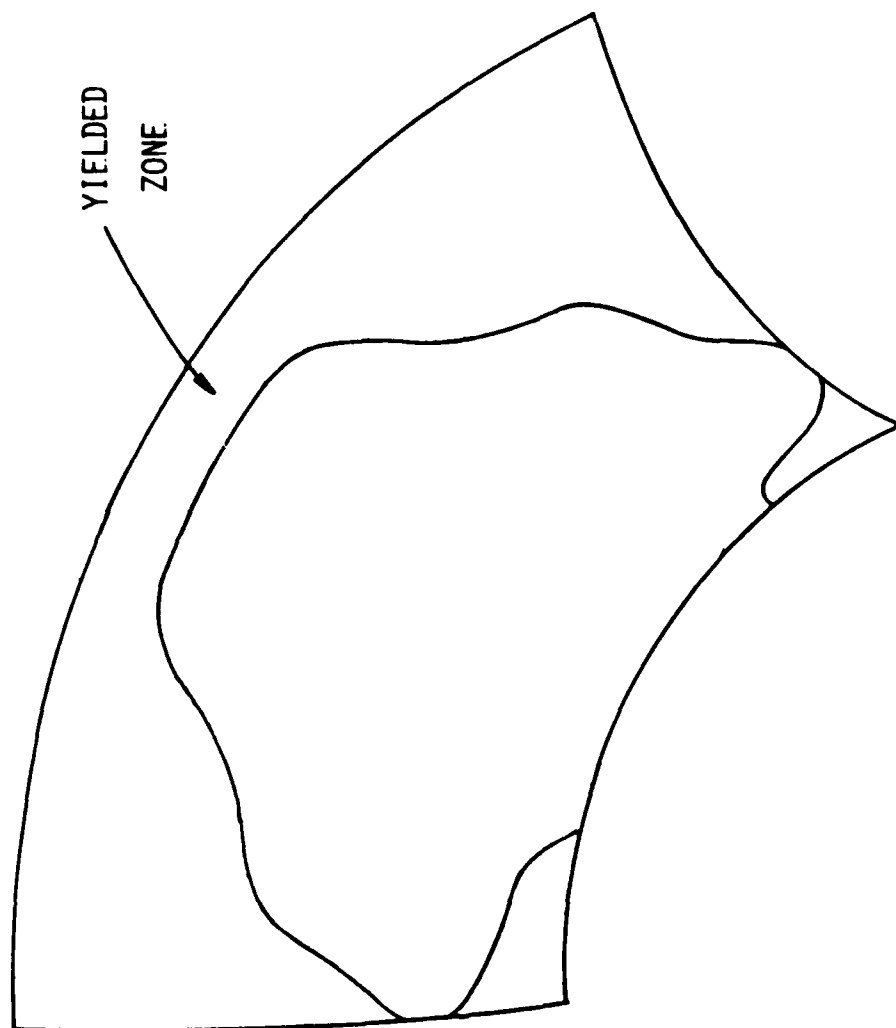


Figure 17. Plastic Boundary in Outer Face Sheet of Toroidal Shell at Maximum Load

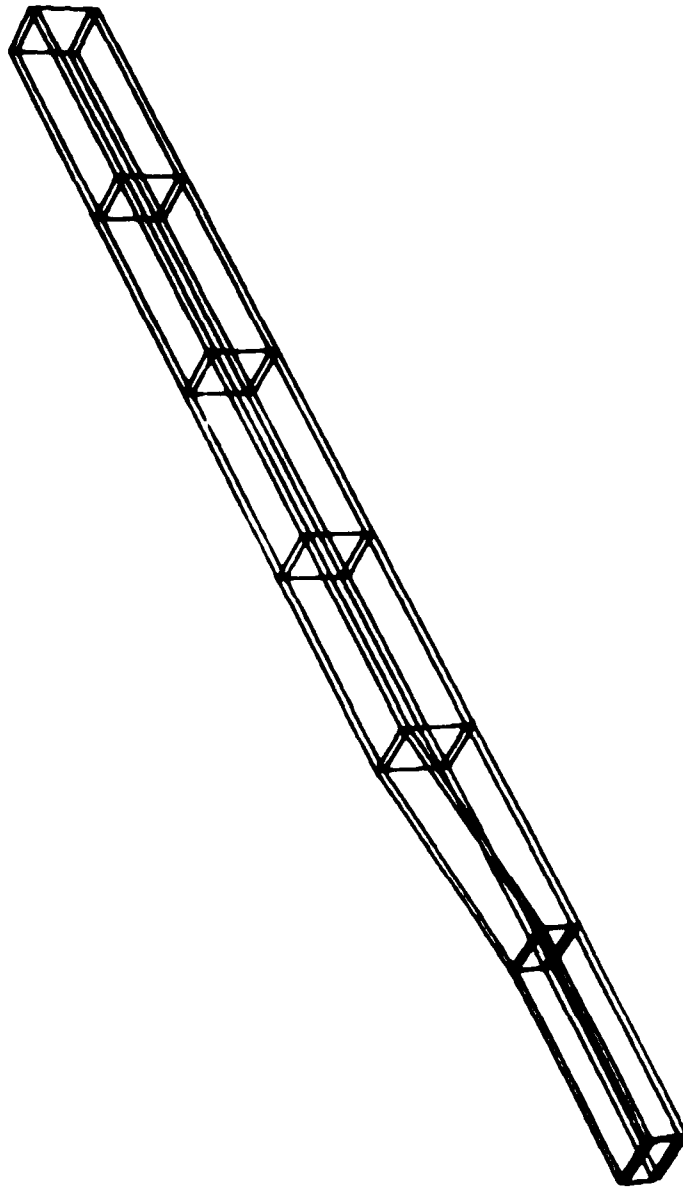


Figure 18. Asymmetric Sandwich Strip.

Face Sheets:  $E = 10. \times 10^6 \text{ lb/in}^2$   
 $\nu = 0.30$   
 $\alpha = 12. \times 10^{-6} \text{ in/in}^\circ\text{F}$   
 Stiffeners:  $E = 10. \times 10^6 \text{ lb/in}^2$   
 $\nu = 0.30$   
 $\alpha = 12.4 \times 10^{-6} \text{ in/in}^\circ\text{F}$   
 Core:  $G_{xz} = 20000. \text{ lb/in}^2$   
 $G_{yz} = 30000. \text{ lb/in}^2$   
 $\alpha_x = \alpha_y = 1. \times 10^{-10} \text{ in/in}^\circ\text{F}$   
 $\alpha_z = 12. \times 10^{-6} \text{ in/in}^\circ\text{F}$

The finite element model of the strip is shown in more detail in Figures 19 and 20. Figure 19 shows the face sheet and full-depth stiffener elements; Figure 20 is a plot of the core layer elements only, in a similar orientation. The model represents only one fourth of the strip due to double symmetry of the problem. The small ends of the strip are fully clamped at all points.

A deformed geometry plot of the panel (Figure 21) after uniform heating shows quite clearly the bending response caused by the asymmetry at the panel ends. The displaced shape (solid lines) is drawn to scale for a temperature rise of  $2000^\circ\text{F}$ . While the deflections remain linear, the transverse central displacement due to uniform temperature rise is approximately  $5.0 \times 10^{-4} \text{ in/}^\circ\text{F}$ .

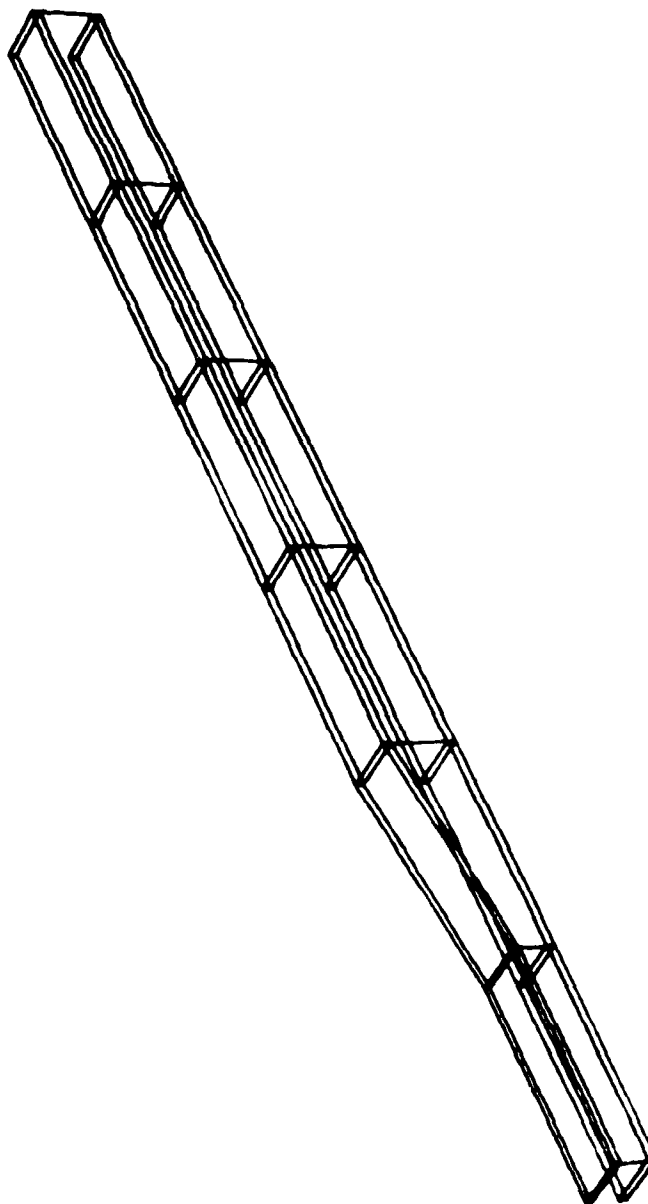


Figure 19. Face Sheet and Stiffener Elements in Sandwich Strip Model.

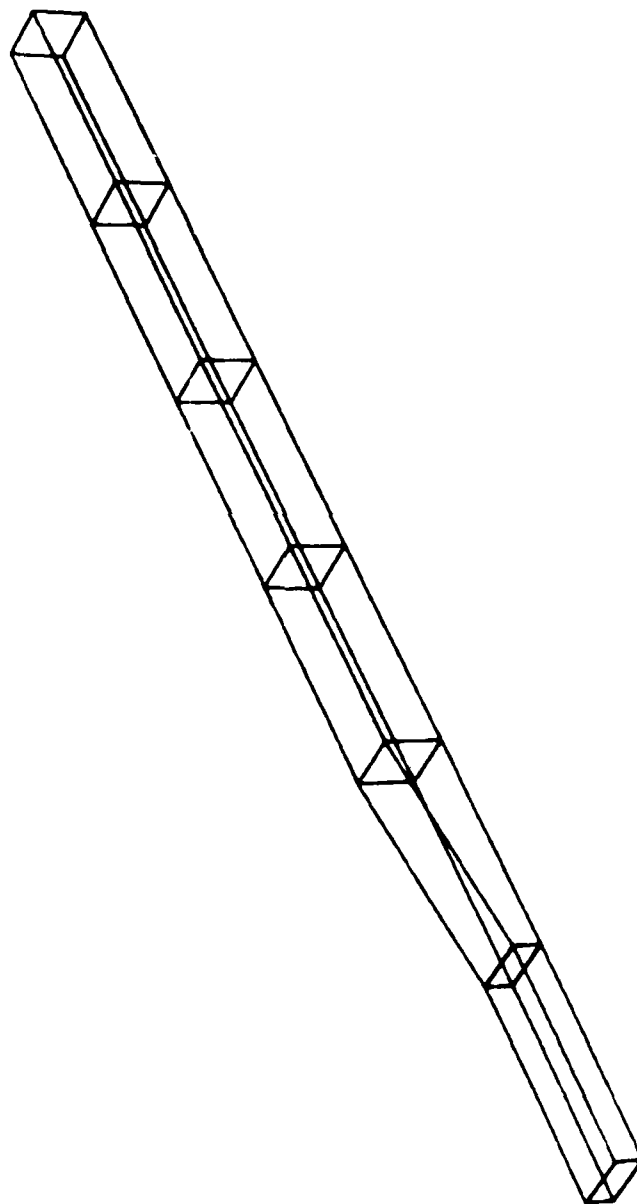


Figure 20. Core Elements in Sandwich Strip Model.

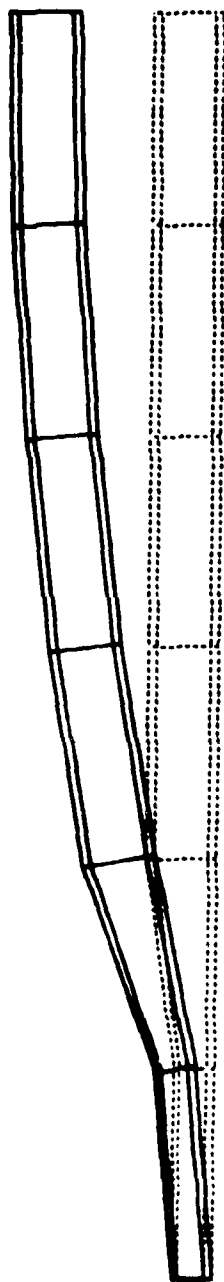


Figure 21. Displaced Shape of Heated Sandwich Strip.

## SECTION 6

### SUMMARY AND CONCLUSIONS

A finite element approach for the linear and nonlinear analysis of structures incorporating sandwich composite materials has been described. The methodology is based upon a philosophy of modeling each layer of a sandwich material in some detail, rather than using approximate properties assembled from the characteristics of each layer. With such an approach, it is a rather straightforward task to simulate response problems involving local deformations, crushing, buckling and plasticity. Furthermore, connections between sandwich panels and other more conventional construction materials may be represented in detail using standard continuum finite elements.

The present formulation includes lower-order thin shell and orthotropic solid elements for representing the basic characteristics of sandwich panels, and compatible bending elements for modeling face sheet or full depth stiffeners. Standard three-dimensional solid elements describe other connected structure, or may be used for more detailed analysis of sandwich panels when required. Each of these elements is applicable to problems involving arbitrarily large displacements or rotations, since no restrictive assumptions are made in the element theoretical formulations. Plasticity is considered using the von Mises yield condition and the Prandtl-Reuss equations of incremental plastic flow.

The finite element approach described has been shown to be effective for numerous applications, involving both mechanical and thermal loading. Natural frequency calculations indicate that the methodology is also quite accurate for this purpose.

## APPENDIX

### COMPUTER PROGRAM INPUT INSTRUCTIONS

The theoretical and numerical formulation described in this report have been implemented in a computer program, from which representative solutions have been presented in Section 5. In the following, input data instructions for use of the program are provided.

The computer program input is divided into 26 input Data Sets, not all of which will be required in a single analysis. Conditions under which each Input Set should be included or skipped are noted at the start of the Data Set. Default values and/or additional explanatory information concerning each item of input are included in each Input Set description in the form of Notes.

For each item of input, a corresponding FORTRAN variable name is listed which serves to define the data type (floating point, integer). Any exceptions to this scheme (e.g., alphanumeric data) are noted explicitly as they occur. All floating point (real) data may be entered with or without exponents; exponents, if used, must be right-justified in the data field provided. Integer value must be input without decimal points or exponents, and must be right-justified in the data field.

No plotting utilities are provided in the present program for display and verification of the finite element model data. For this reason, the nodal coordinate and element connectivity data have been made compatible with that used in the MAGNA finite element program. Therefore, full advantage can be taken of the capabilities offered in the MAGNA program for interactively displaying the model geometry for verification and documentation purposes.

INPUT SET 1

PROBLEM IDENTIFICATION

(Required for all analyses)

CARD	COL	DATA	DESCRIPTION	NOTES
1	1-80	TITLE	Alphanumeric Problem Description	-

# INPUT SET 2

## SOLUTION OPTIONS

(Required for all analyses)

CARD	COL	DATA	DESCRIPTION	NOTES
1	1-5	IATYPE	Analysis Type =1, Linear Static =2, Nonlinear Static =3, Natural Frequency	-
	6-10	ITHERM	Thermal Stress Flag =0, Thermal Stresses Neglected =1, Thermal Stresses Included	-
	11-15	IPØST	Postprocessor File Flag =0, Do Not Save Results =1, Save Analysis Results on File PLOTFIL	-
2	1-5	NINCR	Number of Solution Increments	-
	6-10	IPRNTF	Printing Frequency	-
3	1-10	STEP	Loading Parameter Step Size	(1)

### NOTES:

- (1) In a nonlinear analysis, all external forces are expressed as functions of a "loading parameters," which is continuously increasing during the solution. STEP defines the amount by which the loading parameter (whose initial value is zero) is increased at each solution increment.

# INPUT SET 3

## EQUILIBRIUM ITERATION OPTIONS

(Required only for nonlinear analysis, IATYPE = 2 on input Set 2)

CARD	COL	DATA	DESCRIPTION	NOTES
1	1-5	ITTYPE	Iteration Type =0, No Iteration =1, Modified Newton Iteration =2, Newton-Raphson Iteration	(1)
	6-10	ITFREQ	Iteration Frequency	(2)
	11-15	ITMAX	Maximum Number of Iterations/ Increment	(3)
	16-25	EQTOL	Iteration Convergence Tolerance	(4)

### NOTES:

- (1) ITTYPE determines the type of equilibrium iteration (if any) to be performed at specified intervals in the solution to restore the nonlinear conditions of equilibrium (i.e., internal forces = external forces). Modified Newton-Raphson iteration (ITTYPE = 1) involves no reformulation of the system stiffness matrix; internal forces are computed at each iteration, and the resulting out-of-balance forces are applied to obtain displacement corrections to improve the solution. With full Newton-Raphson iteration (ITTYPE = 2), the stiffness is formed and solved at each iteration. This procedure is, therefore, more expensive than the modified iteration, but is normally quicker to converge.
- (2) Iteration is performed every ITFREQ increments of the nonlinear analysis. The default value is ITFREQ = 1.
- (3) If more than ITMAX iterations are required in any single solution increment, the solution will be terminated to permit a change in increment size or other parameters. The default value is ITMAX = 20.

- (4) EQTØL defines the convergence tolerance on errors in the internal forces  $R$ , as a fraction of the applied load,  $F$ , during equilibrium iteration. The iteration is considered converged when

$$\frac{|| \tilde{F} - \tilde{R} ||}{|| \tilde{F} ||} \leq \text{EQTØL} ,$$

where  $|| \tilde{v} ||$  denotes the Euclidean norm,  $\sqrt{\tilde{v}^T \tilde{v}}$ .

# INPUT SET 4

## EIGENVALUE SOLUTION PARAMETERS

(Required only for natural frequency analysis, IATYPE = 3 in Card Set 2)

CARD	COL	DATA	DESCRIPTION	NOTES
1	1-5	NTRIAL	Number of Iteration Trial Vectors	(1)
	6-10	NREQD	Number of Natural Frequencies to be Determined	(2)
	11-15	MAXIT	Maximum Number of Iterations	(3)
	16-25	TOLVEC	Vector Tolerance for Convergence of Frequency Solution	(4)

### NOTES:

- (1) In general, the greater the number of trial iteration vectors, NTRIAL, the better the convergence and accuracy characteristics of the solution. However, the use of an excessive number of iteration vectors is costly and inefficient in terms of central memory requirements. The use of the  $NTRIAL = \min(2*N, N+5)$ , where N is the number of frequencies to be solved, provides a good balance between rate of convergence and storage requirements. The default value is  $NTRIAL = 2$ .
- (2) The program will determine the first NREQD natural frequencies and normal modes of the linear system  $KX = \omega^2 MX$ , where K is the system stiffness matrix and M the mass matrix. Since the solution is performed by vector iteration, NREQD is limited to values which are relatively small for large finite element models. The default value is  $NREQD = 1$ .
- (3) MAXIT controls the total number of iteration cycles performed during the solution. A value of  $MAXIT = 15$  to 20 is sufficient for nearly all problems, unless the number of frequencies to be computed (NREQD) is quite large. A default value of  $MAXIT = 15$  is used.

- (4) TOLVEC defines the convergence tolerance on successive approximations to each eigenvector. If  $\underline{v}_i$  and  $\underline{v}_{i+1}$  are successive iterates to a single eigenvector, that eigenvector is considered converged if

$$\| \underline{v}_{i+1} - \underline{v}_i \| < \text{TOLVEC} ,$$

where  $\|v\|$  denotes the Euclidean norm,  $\sqrt{y^T y}$ . The default is TOLVEC = 0.001.

# INPUT SET 5

## NODAL COORDINATES

(Required for all analyses)

The number of cards entered in this Section is determined by the number of nodal points to be defined in the model. Nodal input is terminated by a single blank card (i.e., NODE = 0).

CARD	COL	DATA	DESCRIPTION	NOTES
1	1-5		Literal "COORDINATES"	-
	16-20	NODES	Total Number of Node Points	-
	21-25	(blank)		
	26-35	TDFLT	Default Nodal Temperature Value	(1)
	36-40	ITDATA	Load Parameter Curve for Variation of Nodal Temperatures	(2)
2-n	1-5	NODE	Node Point Number	(3)
	6	ISYS	Reference Coordinate System = : Cartesian X,Y,Z, =A: Cylindrical R, $\theta$ ,Z =B: Spherical R, $\phi$ , $\theta$	(4)
	7-10	NINCR	Increment for Node Point Generation	(5)
	11-20	X(NODE)	Coordinate $X_1$	
	21-30	Y(NODE)	Coordinate $X_2$	
	31-40	Z(NODE)	Coordinate $X_3$	
	41-50	T(NODE)	Nodal Temperature	(6)

NOTES:

- (1) TDFLT is a default temperature value which will be assigned to any node point whose input temperature value is zero. This parameter is commonly used in problems of uniform heating, etc., in which temperature data may be absent from the original input data.
- (2) ITDATA refers to a loading parameter curve (i.e., function of time) which is input in input set 25. Curve ITDATA describes the variation of temperature at all nodes in the model, and is used in nonlinear analysis only.
- (3) Acceptable nodal point numbers are between 1 and NODES. Not every node need be connected to an active element in the model, but inactive nodes must be fully constrained (through boundary condition input). Coordinate data is read until a blank (i.e., NODE = 0) is encountered.
- (4) Nodes may be defined in circular cylindrical coordinates by setting ISYS = A and providing as input the R,  $\theta$ , Z coordinates of the point, where  $\theta$  is measured in degrees. In this case, the node coordinates are converted internally to Cartesian coordinates defined by:

$$X = R \cos \theta$$

$$Y = R \sin \theta$$

$$Z = Z.$$

When ISYS = B, the program interprets coordinate data as spherical coordinate values R,  $\phi$ , and  $\theta$ , where both  $\phi$  and  $\theta$  are measured in degrees. Spherical coordinates are then converted to Cartesian coordinates by the formulas:

$$X = R \sin \phi \cos \theta$$

$$Y = R \sin \phi \sin \theta$$

$$Z = R \cos \phi.$$

- (5) Node generation increments NINCR are entered on the second card of a pair, causing nodes to be equally spaced between the last and current nodes, with numbering increment NINCR. As an example, the data

10		0.	0.	0.
20	2	10.	-10.	0.

is equivalent to

10		0.	0.	0.
12		2.	-2.	0.
14		4.	-4.	0.
16		6.	-6.	0.
18		8.	-8.	0.
20		10.	-10.	0.

Note that incremental node generation is performed in the Cartesian system only.

- (6) Nodal temperatures are understood to be the differences in temperature from the (unstressed) reference of the structure (usually "room temperature").

INPUT SET 5

GIZING PARAMETERS FOR SANDWICH CORE ELEMENTS

(Skip this Set if no Sandwich Core Elements are to be defined)

CARD	COL	DATA	DESCRIPTION	NOTES
1	1-5	IECOPE	Element Type Code; Enter the number "2"	-
	6-10	NMAT	Number of Material Property Sets	(1)
	11-15	NELEM	Number of Elements of this Element Type	-
	16-20	NAXIS	Number of Orthotropic Axis Definitions	(2)

NOTES:

- (1) NMAT defines the total number of property sets to be defined in Input Sets 6 and 7.
- (2) NAXIS determines the number of axis sets to be defined in Input Set 8.

# INPUT SET 6

## ISOTROPIC SANDWICH CORE PROPERTIES

(Skip this Set if no Sandwich Core Elements are used)

CARD	COL	DATA	DESCRIPTION	NOTES
1	1-10	EE(I)	Elastic Modulus	(1)
	11-20	PR(I)	Poisson's Ratio	(1)
	21-30	DNS(I)	Mass Density	(2)
	31-40	YLD(I)	Equivalent Stress at First Yield	(3)
	41-50	ALPHA(I)	Coefficient of Thermal Expansion	

### NOTES:

- (1) Repeat Card 1 for each isotropic core material to be defined. The first card defines material property set number 1, the second card, set number 2, and so on. For low-modulus core materials in which the transverse shear moduli are of primary importance, setting  $EE(I) = 2G$  and  $PR(I) = 0$  is usually adequate.
- (2) Mass densities are entered in Force-Length-Time units (weight density/gravity).
- (3) The default value of  $YLD(I)$  is  $1.0 \times 10^{20}$  (elastic core).

INPUT SET 7

ORTHOTROPIC SANDWICH CORE PROPERTIES

(Skip this Set if no Sandwich Core Elements are used)

CARD	COL	DATA	DESCRIPTION	NOTES
1	1	MTYPE	Literal "A" - Flag for Orthotropic Materials Data	(1)
	2-10	E1(I)	Elastic Modulus in Direction 1	-
	11-20	E2(I)	Elastic Modulus in Direction 2	-
	21-30	E3(I)	Elastic Modulus in Direction 3	-
	31-40	G12(I)	Shear Modulus in Plane 1-2	-
	41-50	G13(I)	Shear Modulus in Plane 1-3	-
	51-60	G23(I)	Shear Modulus in Plane 2-3	-
2	1-10	PR12(I)	Poisson's Ratio in Plane 1-2	-
	11-20	PR13(I)	Poisson's Ratio in Plane 1-3	-
	21-30	PR23(I)	Poisson's Ratio in Plane 2-3	-
	31-40	DNS(I)	Mass Density	-
	41-50	ALPHA1(I)	Coefficient of Thermal Expansion in Direction 1	-
	51-60	ALPHA2(I)	Coefficient of Thermal Expansion in Direction 2	-
	61-70	ALPHA3(I)	Coefficient of Thermal Expansion in Direction 3	-

NOTES:

- (1) Repeat Cards 1 and 2 for each orthotropic core material to be defined. Note that all orthotropic materials must be elastic, and are defined with respect to the principal directions of the material.

# INPUT SET 8

## ORTHOTROPIC AXIS DEFINITIONS FOR SANDWICH CORE ELEMENTS

(Skip this Set if no Sandwich Core Elements are used, or if  
NAXIS = 0)

CARD	COL	DATA	DESCRIPTION	NOTES
1	1-5	NODE1(I)	Node Numbers Defining Origin of Coordinates	(1)
	6-10	NODE2(I)	Node Number Defining Material Direction 1	
	11-15	NODE3(I)	Node Number Defining one Additional Point in the 1-2 Plane of the Material	

### NOTES:

- (1) Repeat Card 1 to define NAXIS sets of axis directions. Orthotropic material axes are defined in terms of existing nodes of the finite element model as shown in Figure A.1.

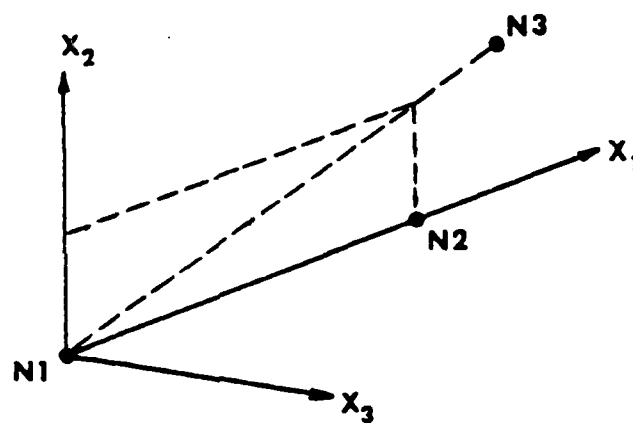


Figure A.1. Orthotropic Axis Definition.

# INPUT SET 9

## ELEMENT CONNECTIVITY, SANDWICH CORE ELEMENTS

(Skip this Set if no Sandwich Core Elements are used)

CARD	COL	DATA	DESCRIPTION	NOTES
1	1-5	IEL	Element Number	(1)
	6-10	IPR	Material Property Set Number for this Element (from Input Set 6 or 7)	-
	11-15	IAX	Orthotropic Axis Set Number (from Input Set 8)	-
	16-20	KGEN	Node Increment for Element Generation	(2)
	21-25	N(1)	Local Node Number 1	(3)
	26-30	N(2)	Local Node Number 2	-
	.	.	.	.
	.	.	.	.
	.	.	.	.
	56-60	N(8)	Local Node Number 8	-

### NOTES:

- (1) Repeat Card 1 as required to define all Sandwich Core Elements. Elements must be entered in ascending order, for IEL = 1,2,...,NELEM. A single blank card is used to terminate this section of input.
- (2) A nonzero value of KGEN on the second card of a pair causes intermediate elements to be generated, by incrementing N(I) by KGEN for each succeeding element. More than one element must be generated to use this feature.
- (3) Node point ordering for the Sandwich Core Element is shown in Figure A.2.

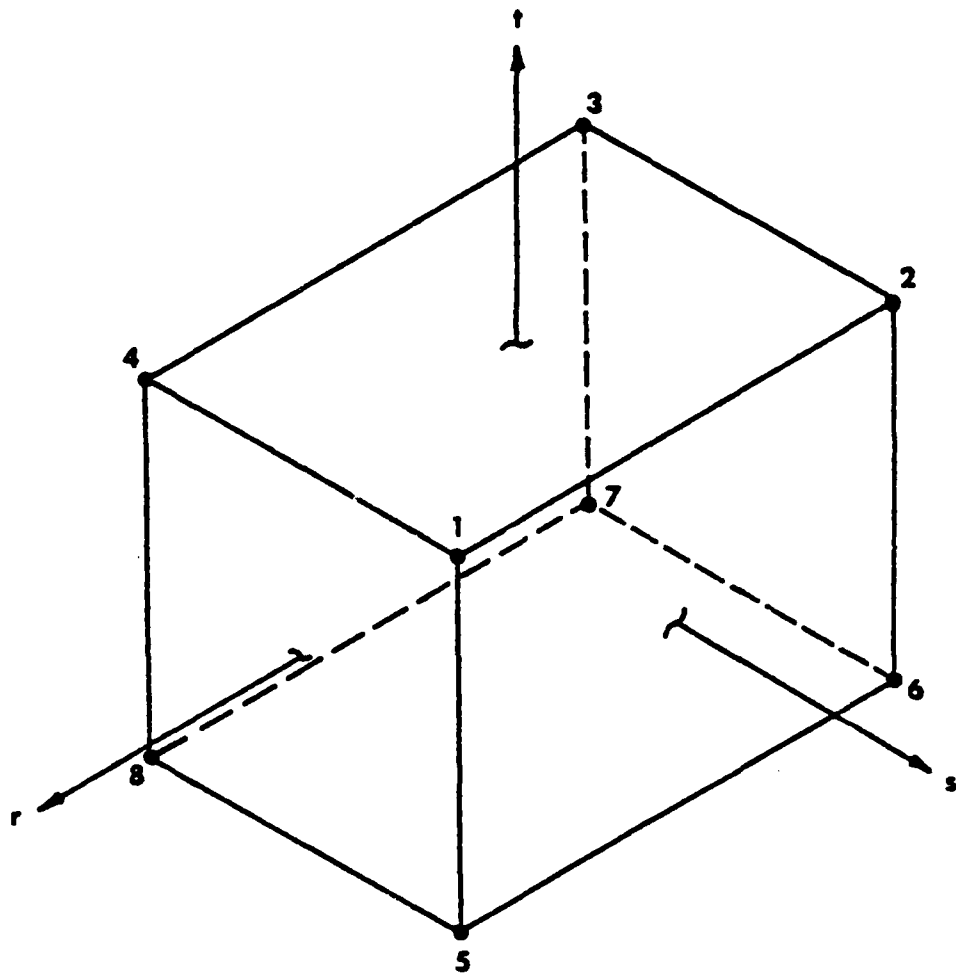


Figure A.2. Connectivity for Sandwich Core Element.

INPUT SET 10

SIZING PARAMETERS FOR STIFFENER ELEMENTS

(Skip this Set if no Stiffener Elements are to be defined)

CARD	COL	DATA	DESCRIPTION	NOTES
1	1-5	IECODE	Element Type Code; Enter the Number "3"	-
	6-10	NMAT	Number of Material Property Sets (Maximum of 20)	-
	11-15	NELEM	Number of Elements of this Element Type	-

# INPUT SET 11

## STIFFENER ELEMENT PROPERTIES

(Skip this Set if no Stiffener Elements are used)

CARD	COL	DATA	DESCRIPTION	NOTES
1	1-10	EE(I)	Elastic Modulus	(1)
	11-20	PR(I)	Poisson's Ratio	(1)
	21-30	DNS(I)	Mass Density	(2)
	31-40	YLD(I)	Equivalent Stress at First Yield	(3)
	41-50	ALPHA(I)	Coefficient of Thermal Expansion	

### NOTES:

- (1) Repeat Card 1 for each stiffener material to be defined. The first line entered in this Input Set defines stiffener property set number 1, the second line defines property set 2, and so on. Note that, for face sheet stiffeners (i.e., slender beams), it is appropriate to set the Poisson's Ratio, PR(I), to zero.
- (2) Mass densities are entered in Force-Length-Time units (weight/density/gravity).
- (3) The default value of YLD(I) is  $1.0 \times 10^{20}$  (elastic material).

# INPUT SET 12

## CONNECTIVITY FOR STIFFENER ELEMENTS

(Skip this Set if no Stiffener Elements are used)

CARD	COL	DATA	DESCRIPTION	NOTES
1	1-5	IEL	Element Number	(1)
	6-10	(Blank)		
	11-15	IPR	Material Property Set for this Element	-
	16-20	(Blank)		
	21-25	KGEN	Node Increment for Element Generation	(2)
	26-30	N(1)	Local Node Number 1	(3)
	31-35	N(2)	Local Node Number 2	
	36-40	N(3)	Local Node Number 3	
	41-45	N(4)	Local Node Number 4	
	46-55	THICK	Stiffener Width or Depth	(4)

### NOTES:

- (1) Repeat Card 1 as required to define all Stiffener Elements. Face sheet and full-depth stiffeners may be intermixed freely. All elements must be entered in ascending order, with a single blank line entered to terminate input.
- (2) A nonzero value of KGEN on the second card of a pair causes intermediate elements to be generated, by incrementing N(I) by KGEN for each succeeding element. More than one element must be generated to use this feature.
- (3) Node point ordering for all Stiffener Elements is shown in Figure A.3. N(1) through N(4) are the global node numbers corresponding to positions 1 through 4 in the Figure.

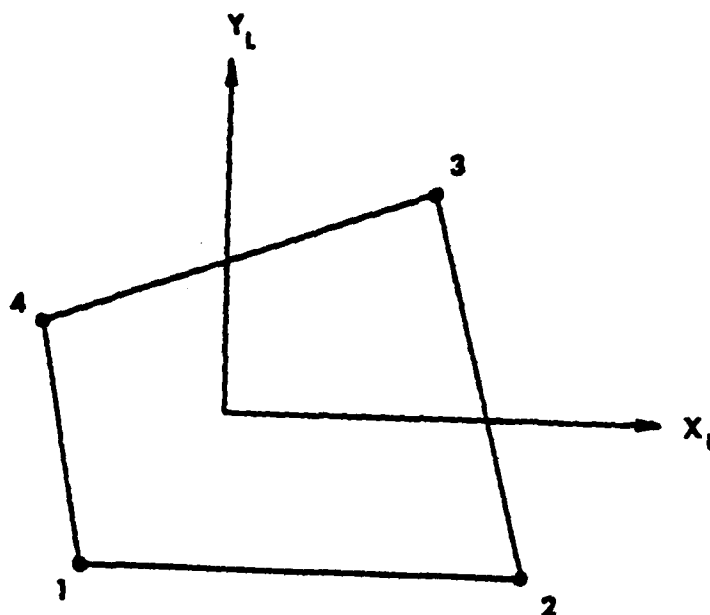


Figure A.3. Connectivity for Stiffener Elements.

- (4) The Stiffener Element depth is defined by the positions of its connected nodes. THICK is the element dimension perpendicular to the warped plane defined by nodes N(1) through N(4).

INPUT SET 13

SIZING PARAMETERS FOR THIN SHELL ELEMENTS

(Skip this Set if no Thin Shell Elements are to be defined)

CARD	COL	DATA	DESCRIPTION	NOTES
1	1-5	IECODE	Element Type Code; Enter the Number "5"	-
	6-10	NMAT	Number of Material Property Sets (Maximum of 20)	-
	11-15	NELEM	Number of Elements of this Element Type	-

INPUT SET 14

THIN SHELL MATERIAL PROPERTIES

(Skip this Set if no Thin Shell Elements are used)

CARD	COL	DATA	DESCRIPTION	NOTES
1	1-10	EE(I)	Elastic Modulus	(1)
	11-20	PR(I)	Poisson's Ratio	-
	21-30	DNS(I)	Mass Density	(2)
	31-40	ALPHA(I)	Coefficient of Thermal Expansion	-

NOTES:

- (1) Repeat Card 1 for each Thin Shell material to be defined.
- (2) Mass densities are entered in Force-Length-Time units (weight density/gravity).

# INPUT SET 15

## THIN SHELL ELEMENT CONNECTIVITY

(Skip this Set of no Thin Shell Elements are used)

CARD	COL	DATA	DESCRIPTION	NOTES
1	1-5	IEL	Element Number	(1)
	6-10	IPR	Material Property Set for this Element	-
	11-15	KGEN	Node Increment for Element Generation	(2)
	16-20	N(1)	Local Node Number 1	(3)
	21-25	N(2)	Local Node Number 2	
	.	.	.	
	.	.	.	
	.	.	.	
	51-55	N(8)	Local Node Number 8	-

### NOTES:

- (1) Repeat Card 1 as required to define all Thin Shell Elements. Elements must be entered in ascending order for IEL = 1,2,..., NELEM. A single blank card terminates this section of input.
- (2) A nonzero value of KGEN on the second card of a pair causes intermediate elements to be generated, by incrementing N(I) by KGEN for each succeeding element. More than one element must be generated to use this feature.
- (3) Node point ordering for the Thin Shell Element is shown in Figure A.4.

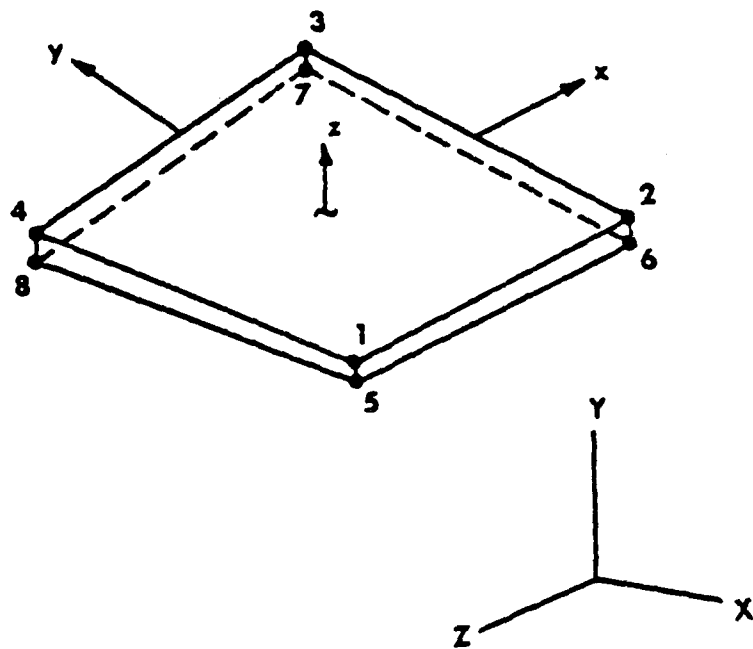


Figure A.4. Connectivity for Thin Shell/Face Sheet Element.

INPUT SET 16

SIZING PARAMETERS FOR 3-D SOLID ELEMENTS

(Skip this Set if no Solid Elements are to be defined)

CARD	COL	DATA	DESCRIPTION	NOTES
1	1-5	IECODE	Element Type Code; Enter the Number "7"	-
	6-10	NMAT	Number of Material Property Sets	(1)
	11-15	NELEM	Number of Elements of this Element Type	-
	16-20	NAXIS	Number of Orthotropic Axis Definitions	(2)

NOTES:

- (1) NMAT defines the total number of property sets to be defined in Input Sets 17 and 18.
- (2) NAXIS determines the number of axis sets to be defined in Input Set 19.

AD-A106 378

DAYTON UNIV OH RESEARCH INST

F/G 11/4

NONLINEAR FINITE ELEMENT ANALYSIS OF SANDWICH COMPOSITES. (U)

MAR 81 R A BROCKMAN

F33615-77-C-3075

UNCLASSIFIED

UDR-TR-80-113

AFWAL-TR-81-3008

NL

2 of 2  
Pages



END

DATE  
FILMED  
11-81  
DTIC

**INPUT SET 17**

**ISOTROPIC PROPERTIES FOR 3-D SOLID ELEMENTS**

(Skip this Set if no Solid Elements are used)

CARD	COL	DATA	DESCRIPTION	NOTES
1	1-10	EE(I)	Elastic Modulus	(1)
	11-20	PR(I)	Poisson's Ratio	-
	21-30	DMS(I)	Mass Density	(2)
	31-40	YLD(I)	Equivalent Stress at First Yield	(3)
	41-50	ALPHA(I)	Coefficient of Thermal Expansion	-

**NOTES:**

- (1) Repeat Card 1 for each isotropic material to be defined.
- (2) Mass densities are entered in Force-Length-Time units (weight density/gravity).
- (3) The default value of YLD(I) is  $1.0 \times 10^{20}$  (elastic material).

**INPUT SET 18**

**ORTHOTROPIC PROPERTIES FOR 3-D SOLID ELEMENTS**

(Skip this Set if no Solid Elements are used)

CARD	COL	DATA	DESCRIPTION	NOTES
1	1	MTYPE	Literal "A" - Flag for Orthotropic Materials Data	-
	2-10	E1(I)	Elastic Modulus in Direction 1	-
	11-20	E2(I)	Elastic Modulus in Direction 2	-
	21-30	E3(I)	Elastic Modulus in Direction 3	-
	31-40	G12(I)	Shear Modulus in Plane 1-2	-
	41-50	G13(I)	Shear Modulus in Plane 1-3	-
	51-60	G23(I)	Shear Modulus in Plane 2-3	-
2	1-10	PR12(I)	Poisson's Ratio in Plane 1-2	-
	11-20	PR13(I)	Poisson's Ratio in Plane 1-3	-
	21-30	PR23(I)	Poisson's Ratio in Plane 2-3	-
	31-40	DNS(I)	Mass Density	-
	41-50	ALPHA1(I)	Coefficient of Thermal Expansion in Direction 1	-
	51-60	ALPHA2(I)	Coefficient of Thermal Expansion in Direction 2	-
	61-70	ALPHA3(I)	Coefficient of Thermal Expansion in Direction 3	-

**NOTES:**

- (1) Repeat Cards 1 and 2 for each orthotropic solid material to be defined. Note that all orthotropic materials must be elastic, and are defined with respect to the principal directions of the material.

# INPUT SET 19

## ORTHOTROPIC AXIS DEFINITIONS FOR 3-D SOLID ELEMENTS

(Skip this Set if no Solid Elements are used, or if NAXIS = 0)

CARD	COL	DATA	DESCRIPTION	NOTES
1	1-5	NODE1(I)	Node Number Defining Origin of Coordinates	(1)
	6-10	NODE2(I)	Node Number Defining Material Direction 1	
	11-15	NODE3(I)	Node Number Defining one Additional Point in the 1-2 Plane of the Material	

### NOTES:

- (1) Repeat Card 1 to define NAXIS sets of axis directions. Orthotropic material axes are defined in terms of existing nodes of the finite element model as shown in Figure A.1.

**INPUT SET 20**

**CONNECTIVITY FOR 3-D SOLID ELEMENTS**

(Skip this Set if no Solid Elements are used)

CARD	COL	DATA	DESCRIPTION	NOTES
1	1-5	IEL	Element Number	(1)
	6-10	IPR	Material Property Set for this Element	-
	11-13	IAX	Orthotropic Axis Set	-
	14-15	INT	Order of Numerical Integration	(2)
	16-20	KGEN	Node Increment for Element Generation	(3)
	21-25	(Blank)		
	26-30	N(1)	Local Node Number 1	(4)
	31-35	N(2)	Local Node Number 2	-
	.	.	.	.
	.	.	.	.
2	75-80	N(11)	Local Node Number 11	
	1-5	N(12)	Local Node Number 12	-
	6-10	N(13)	Local Node Number 13	-
	.	.	.	.
	.	.	.	.
	.	.	.	.
	41-45	N(20)	Local Node Number 20	-

**NOTES:**

- (1) Repeat Cards 1 and 2 as required to define all Solid Elements. Elements must be entered in ascending order for IEL = 1,2,..., NELEM. A single blank card is used to terminate this section of input.
- (2) Acceptable values for INT are INT = 2 (2 by 2 by 2 Gaussian integration) and INT = 3 (3 by 3 by 3 Gaussian integration).
- (3) A nonzero value of KGEN on the second card of a pair causes intermediate elements to be generated, by incrementing N(I) by KGEN for each succeeding element. More than one element must be generated to use this feature.
- (4) Node point ordering for the Solid Element is shown in Figure A.5. Note that nodes 1-8 are always required, but nodes 9-20 may each be included or omitted as desired.

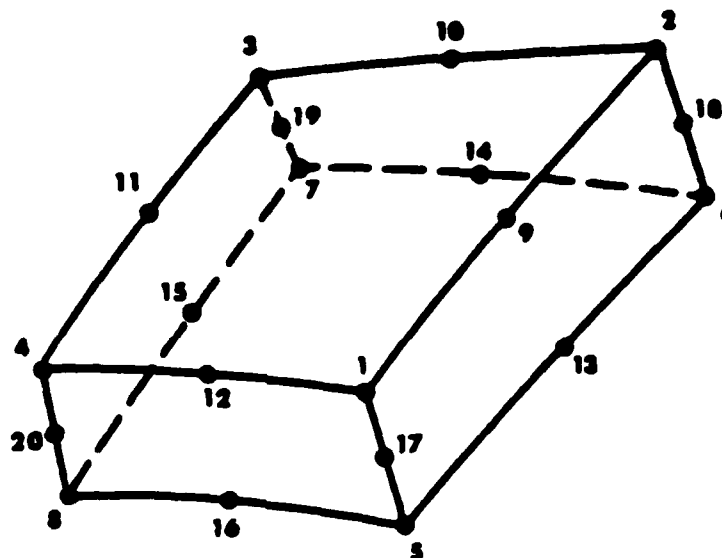


Figure A.5. Connectivity for 3-D Solid Element.

**INPUT SET 21**

**ELEMENT INPUT TERMINATOR**

(Required for all analyses)

CARD	COL	DATA	DESCRIPTION	NOTES
1	1-80	(blank)		(1)

**NOTES:**

- (1) This input line terminates element input for the problem being defined, and is required for all analysis options.

**INPUT SET 22**

**SIZING PARAMETERS FOR BOUNDARY CONDITION DATA**

**(Required for all analyses)**

CARD	COL	DATA	DESCRIPTION	NOTES
1	1-5	NB(1)	Number of Type 1 Boundary Conditions	(1)
	6-10	NB(2)	Number of Type 2 Boundary Conditions	(2)

**NOTES:**

- (1) Type 1 and Type 2 boundary conditions are defined in Input Sets 23 and 24, respectively.

# INPUT SET 23

## BOUNDARY CONDITIONS, TYPE 1

(Skip this Set if NB(1) = 0 in Input Set 22)

Boundary conditions entered in this Input Set are used to constrain a range of nodes in specified coordinate directions.

CARD	COL	DATA	DESCRIPTION	NOTES
1	1-5	N1	Beginning Node Number	(1)
	6-10	N2	Ending Node Number	-
	11-15	INCR	Node Number Increment	-
2	1-5	JD(1)	First Direction Constrained	(1)
	6-10	JD(2)	Second Direction Constrained	-
	11-15	JD(3)	Third Direction Constrained	-

### NOTES:

- (1) Repeat Cards 1 and 2 NB(1) times to define all Type 1 boundary conditions. Nodes N1, N1 + INCR, N1 + 2\*INCR, ... N2 will be constrained in the directions JD(I); I = 1,2,3. One or more of the JD(I) may be zero. Valid nonzero entries for JD(I) are 1,2,3 for constraints in the x,y and z directions respectively.

# INPUT SET 24

## BOUNDARY CONDITIONS, TYPE 2

(Skip this Set if NB(2) = 0 in Input Set 22)

Boundary conditions entered in this Input Set are used to constrain an arbitrary list of nodes in specified coordinate directions.

CARD	COL	DATA	DESCRIPTION	NOTES
1	1-5	JD(1)	First Direction Constrained	(1)
	6-10	JD(2)	Second Direction Constrained	-
	11-15	JD(3)	Third Direction Constrained	-
2	1-5	ND(1)	First Node Constrained	(1)
	6-10	ND(2)	Second Node Constrained	-
	.	.	.	.
	.	.	.	.
	.	.	.	.
	46-50	ND(10)	Tenth Node Constrained	-

### NOTES:

- (1) Repeat Cards 1 and 2 NB(2) times to define all Type 2 boundary conditions. The nodes ND(I); I = 1,...,10 will each be constrained in the directions specified by the JD(I). Some of the directions (JD's) and some of the nodes (ND's) may be zero.

# INPUT SET 25

## NONLINEAR LOADING FUNCTIONS

(Required for nonlinear analyses only)

Loading and/or temperature variations are defined in this Set as functions of a single independent loading parameter, which is continually increasing during the solution.

CARD	COL	DATA	DESCRIPTION	NOTES
1	1-5	NFUNCT	Number of Loading Functions to be Defined	(1)
2	1-5	IFUNCT	Load Function Identification Number	(2)
	6-10	NPTS	Number of Point Pairs [X(I), Y(I)] Used to Define the Curve	(3)
	11-80	TITL	Optional Alphanumeric Title	
3	1-10	X(1)	Abscissa for First Data Point	-
	11-20	Y(1)	Ordinate for First Data Point	-
	.	.	.	
	.	.	.	
	.	.	.	
	61-70	X(4)	Abscissa for Fourth Data Point	-
	71-80	Y(4)	Ordinate for Fourth Data Point	
4-7	1-80		Additional Pairs [X(I),Y(I)] as shown for Card 3	(4)

NOTES:

- (1) More than one loading function will be needed only if non-proportional loads are to be considered in the analysis. A maximum of fifty loading functions may be defined.
- (2) Loading functions must be numbered between 1 and 50 inclusive. The functions need not be numbered sequentially, nor must they be entered in any particular order.
- (3) Up to 20 data points may be used to define each load function. Each data point is defined by an abscissa (the loading parameter value  $X(I)$ ) and an ordinate (the function value  $Y(I)$ ).
- (4) Cards 4-7 are required for a given loading function only if the number of points exceeds four. Unneeded cards should not be entered.

# INPUT SET 26

## APPLIED LOADING

(Required for linear and nonlinear static analyses)

CARD	COL	DATA	DESCRIPTION	NOTES
1	1-5	NODE	Node at which Load is Applied	(1)
	6-10	IDIR	Direction of Loading (1=X, 2=Y, 3=Z)	-
	11-15	NCURV	Identification Number of Loading Function Describing the Variation of the Load	(2)
	16-25	SCALE	Scale Factor or Load Magnitude	(3)

### NOTES:

- (1) Repeat Card 1 as required to define all applied forces acting on the model. Loads may be entered in any order. Input in this section is terminated by a single blank card.
- (2) The history of each load during the solution is determined by one of the loading functions entered in Input Set 25. The parameter NCURV is ignored in linear analysis.
- (3) In linear analysis, SCALE is the actual magnitude of force to be applied at the given node in the specified direction. For nonlinear problems, the value obtained from the specified loading function (NCURV) at any stage of the solution will be multiplied by the value of SCALE.

## REFERENCES

1. O. C. Zienkiewicz, The Finite Element Method, McGraw-Hill, 1979.
2. G. R. Monforton, "Discrete Element, Finite Displacement Analysis of Anisotropic Sandwich Shells," Report No. 39, Division of Solid Mechanics, Structures and Mechanical Design, Case Western Reserve University, 1970.
3. R. A. Brockman, "Finite Element Method for the Finite Displacement Analysis of Sandwich Composite Panels," AFFDL-TR-78-14, Wright-Patterson Air Force Base, Ohio, 1978.
4. J. B. Kennedy, "On the Deformation of Parallelogrammic Sandwich Panels," The Aeronautical Journal, Royal Aeronautical Society, June 1970.
5. P. Sharifi, "Nonlinear Analysis of Sandwich Structures," Ph.D. Dissertation, University of California, Berkeley, 1970.
6. R. D. Cook, "Two Hybrid Elements for the Analysis of Thick, Thin, and Sandwich Plates," International Journal for Numerical Methods in Engineering, Vol. 5, pp. 277-288, 1972.
7. L. E. Malvern, Introduction to the Mechanics of a Continuous Medium, Prentice-Hall, 1969.
8. R. M. Jones, Mechanics of Composite Materials, Scripta Book Co., Washington, D.C., 1975.
9. A. Mendelson, Plasticity: Theory and Applications, MacMillan, New York, 1968.
10. B. Hunsaker, W. E. Haisler, and J. A. Stricklin, "On the Use of Two Hardening Rules of Plasticity in Incremental and Pseudo-Force Analysis," in Constitutive Equations in Viscoplasticity: Computational and Engineering Aspects, AMD Volume 20, ASME Publications, New York, 1976.
11. R. A. Brockman, "A Penalty Function Approach for the Non-linear Finite Element Analysis of Thin Shells," Ph.D. Dissertation, Dept. of Mechanical Engineering, University of Dayton, Dayton, Ohio, July 1979.
12. Y. C. Fung, Foundations of Solid Mechanics, Prentice-Hall, 1965.
13. R. B. Coor and A. Jennings, "A Simultaneous Iteration Algorithm for Symmetric Eigenvalue Problems," International Journal for Numerical Methods in Engineering, Vol. 10, pp. 647-663, 1976.

14. H. P. Kan and J. C. Huang, "Large Deflections of Rectangular Sandwich Plates," AIAA Journal, Vol. 5, pp. 1706-1708, 1967.
15. F. J. Plantema, Sandwich Construction, John Wiley and Sons, 1966.
16. W. J. Hoff, "Bending and Buckling of Rectangular Sandwich Plates," NACA-TN-225, 1950.
17. R. A. Brockman, "Stability of Flat, Simply-Supported Rectangular Sandwich Panels Subjected to Combined Inplane Loadings," AFFDL-TR-76-14, Wright-Patterson Air Force Base, Ohio, 1976.
18. K. H. Boller, "Buckling Loads of Flat Sandwich Panels in Compression: The Buckling of Flat Sandwich Panels with Edges Simply Supported," Report No. 1525-A, Forest Products Laboratory, Madison, Wisconsin, 1947.
19. R. A. Brockman, "MAGNA Computer Program User's Manual," UDR-TR-80-107, University of Dayton Research Institute, Dayton, Ohio, November, 1980.

EN  
DAT  
FILM